NASA CONTRACTOR REPORT


NASA CR-2807



# NSEG - A SEGMENTED MISSION ANALYSIS PROGRAM FOR LOW AND HIGH SPEED AIRCRAFT

## Volume I - Theoretical Development

| 1. Report No. | 2. Government Accession No. | 3. Recipient's Catalog No. |
|---|---|---|
| NASA CR-2807 | | |

| 4. Title and Subtitle | 5. Report Date |
|---|---|
| NSEG - A Segmented Mission Analysis Program for Low and High Speed Aircraft. Volume I - Theoretical Development | August 1977 |
| | 6. Performing Organization Code |
| 7. Author(s) | 8. Performing Organization Report No. |
| D. S. Hague and H. L. Rozendaal | |
| | 10. Work Unit No. |
| 9. Performing Organization Name and Address | 11. Contract or Grant No. |
| Aerophysics Research Corporation<br>Bellevue, WA 98009 | NAS1 - 13599 |
| | 13. Type of Report and Period Covered |
| 12. Sponsoring Agency Name and Address | Contractor Report |
| National Aeronautics and Space Administration<br>Washington, D.C. | 14. Sponsoring Agency Code |

15. Supplementary Notes

Langley Technical Monitor: Walter A. Vahl

Volume I of Final Report

16. Abstract

Program NSEG is a rapid mission analysis code based on the use of approximate flight path equations of motion. Equation form varies with the segment type, for example, accelerations, climbs, cruises, descents, and decelerations. Realistic and detailed vehicle characteristics are specified in tabular form. In addition to its mission performance calculation capabilities, the code also contains extensive flight envelope performance mapping capabilities. For example, rate-of-climb, turn rates, and energy maneuverability parameter values may be mapped in the Mach-altitude plane. Approximate take off and landing analyses are also performed. At high speeds, centrifugal lift effects are accounted for. Extensive turbojet and ramjet engine scaling procedures are incorporated in the code.

| 17. Key Words (Suggested by Author(s)) | 18. Distribution Statement |
|---|---|
| Mission Analysis; Trajectories; Air-breathing Propulsion, Turbojets; Ramjets | Unclassified - Unlimited<br><br>Subject Category 01 |

| 19. Security Classif. (of this report) | 20. Security Classif. (of this page) | 21. No. of Pages | 22. Price* |
|---|---|---|---|
| Unclassified | Unclassified | 82 | $5.00 |

*For sale by the National Technical Information Service, Springfield, Virginia 22161

TABLE OF CONTENTS

TABLE OF CONTENTS

TABLE OF CONTENTS

LIST OF FIGURES

# PREFACE

The NSEG program was originally constructed by Mr. L. H. Leet of the United States Air Force Aeronautical Systems Division, Wright-Patterson Air Force Base. The code was subsequently modified and extended by Aerophysics Research Corporation under contract F33615-73-C-3039. The current version of the NSEG (Version III) extends the program applicability to higher speed (hypersonic turbo-ramjet) aircraft. It also includes various improvements generated by Mr. David T. Johnson of the Air Force Flight Dynamics Laboratory. The authors wish to extend their thanks to Mr. Walter Vahl of NASA for his extensive assistance during formulation and checkout of the turbo-ramjet propulsion system model now available in NSEG. The analytic basis of the turbo-ramjet model is due to Mr. Vahl.

Mr. D. S. Hague of Aerophysics Research Corporation served as project leader for the present study. Dr. H. L. Rozendaal provided specialist support in the fields of propulsion system analysis and computer sciences. Mr. R. T. Jones, formerly of Aerophysics Research Corporation, has also made significant contributions to the NSEG code in studies preceding the present one.

Additional details and copies of the program deck can be obtained from NASA Langley Research Center.

# NSEG - A SEGMENTED MISSION ANALYSIS PROGRAM FOR LOW AND HIGH SPEED AIRCRAFT

D. S. Hague and H. L. Rozendaal

*AEROPHYSICS RESEARCH CORPORATION*

## SUMMARY

Program NSEG is a rapid mission analysis code based on the use of approximate flight path equations of motion. Equation form varies with the segment type, for example, accelerations, climbs, cruises, descents, and decelerations. Realistic and detailed vehicle characteristics are specified in tabular form and a variety of layered atmosphere options are available. The mission specification is open-ended in that the upper limit on the number of flight segments to be included in a mission profile (currently one hundred and forty-nine) can be increased by increasing the size of a single common block (CØMTAB) above its current size of 3000 words. The code contains an English language oriented input procedure for describing the mission segment sequence to be employed. In addition to its mission performance calculation capabilities the code also contains extensive flight envelope performance mapping capabilities. For example, rate-of-climb, turn rates, and energy maneuverability parameter values may be mapped in the Mach-altitude plane. Where suitable graphics capabilities exist these maps may be drawn by machine in the form of contour plots.

The code contains several approximate flight path optimization capabilities based on Rutowski energy-like criteria. These flight path optimization formulations permit inclusion of minimum time or fuel flight segments and maximum range segments during climb or descent segments. Approximate take off and landing analyses are also performed. At high speeds centrifugal lift effects are accounted for. Extensive turbojet and ramjet engine scaling procedures are incorporated in the code. Take off and landing analyses are also available which employ a high lift aerodynamic analysis model based on the Air Force Flight Dynamics Laboratory DATCOM method. Alternatively, user supplied high lift aerodynamics can be employed.

This report is Volume I of 3 volumes. Total program documentation consists of:

Volume I. Theoretical Development

Volume II. Program User's Manual

Volume III. Test Problems

# 1. INTRODUCTION

The NSEG code was originally developed by the Air Force and then modified under Air Force Contract F33615-71-C-1480 and subsequently extended to higher speed flight under the present study. Major changes made to NSEG are a complete code reorganization, more general vehicle specification, addition of energy maneuverability concepts, addition of plotting capability, development of new data input procedures, introduction of turbojet and ramjet scaling procedures and the accounting for centrifugal lift effect.

NSEG provides a generalized mission performance analysis capability based on approximate equations of motion for the state components.

$$\{X_i\} = \{V, h, \gamma, W, R, t\} \tag{1}$$

In all flight modes the equations of motion

$$\{\dot{X}_i\} = \{f_i(V, h, \gamma, W, R, t; \alpha, B_A, N)\} \tag{2}$$

are of an approximate nature. For example, in climbs, $\dot{\gamma}$ is neglected.

Approximate equations of motion are available for

1. Take-off
2. Acceleration
3. Climb
4. Cruise and loiter
5. Descent
6. Deceleration
7. Landing

Any number of mission segments may be pieced together to form a complete mission. Segments may be flown in either forward or reverse direction in any sequence specified by the user. This feature allows a direct solution to many two- or N-point boundary condition problems.
A typical complete mission profile is illustrated in Figure (1). The program may also be used to generate performance contour plots of the type illustrated in Figure (2). NSEG contains a variety of operating modes to aid in mission analysis which include

1. *Point performance* characteristic evaluation where given $\{\bar{X}\} = \{X_i\}$ , the function

$$\phi = \phi(X_i) \tag{3}$$

is evaluated.

2. *Vector performance* evaluation where given

$$\{\bar{X}\} = \{\ldots\ldots, X_i, X_j, \ldots\ldots\} \qquad j = 1, 2, \ldots, N_j \tag{4}$$

the vector

$$\{\phi\} = \{\phi_j\} = \{f\ldots, X_i, X_j, \ldots\} \; j = 1, 2, \ldots, N_j \tag{5}$$

is evaluated and the maximum or minimum value of $\phi$ in the region

$$X_{j_L} < X_j < X_{j_H} \tag{6}$$

is found by interpolation. That is,

$$\phi_j^* = f(\ldots, X_i, X_j^*, \ldots) \tag{7}$$

3. *Map performance* evaluation where given

$$\{\bar{X}\}_{ij} = \{\ldots, X_i, X_j, \ldots\} \qquad i = 1, 2, \ldots, N_i$$

$$j = 1, 2, \ldots, N_j \tag{8}$$

the performance array

$$[\phi_{ij}] = [f(\ldots, X_i, X_j, \ldots)] \tag{9}$$

is evaluated over a rectangular mesh of points in the $(X_i, X_j)$ plane and the resulting contours obtained in the manner of Figure (2).

4. *Mission segment performance* where given a state $\{\bar{X}\}$, an approximate state equation, and a segment termination criteria, the state transformation, $T_{ij}$, which transform state i into state j according to

$$\{X\}_i \rightarrow T_{ij} \rightarrow \{\bar{X}\}_j \tag{10}$$

is accomplished.

5. Mission performance where given a sequence of mission segments, the successive state transformations

$$\{\bar{X}\}_1 \rightarrow \{\bar{X}\}_2 \rightarrow \quad \ldots \quad \rightarrow \{\bar{X}_{N-1}\} \rightarrow \{\bar{X}_N\} \tag{11}$$

are completed.

The analytic basis of program NSEG is presented below. Section 2 describes the propulsion system characterizations available. Aerodynamics are described in Section 3. Sections 4 and 5 present the vehicle weight model and the planetary representation. Section 6 describes the mission segment transformation calculation and Section 7 the mission segment options which use the transformations. Program mapping capabilities are described in Section 8.

Constants utilized in the NSEG code employ English Units (lb., ft., sec., naut. mi., and degrees Rankine) exclusively. It is imperative therefore that input quantities employ English Units; constants utilized in the illustrations reproduced in the text reflect this convention. Provisions of NASA Policy Directive (NPD 220.4) have been waived for those portions of this report that pertain to the NSEG computer code.

# 2. PROPULSION

## 2.1 Simplified Propulsion Systems

All propulsive representations compute the vehicle fuel flow rate given a flight condition and the required thrust. Vehicle required thrust is computed internally by NSEG on the basis of instantaneous flight conditions.

The maximum thrust, $T_{max}$, is given by

$$T_{max} = T_{max1}, T_{max2}, \text{ or } T_{max3} \tag{12}$$

where

$$T_{maxj} = T_{maxj}(M, h) \tag{13}$$

A throttle parameter, N, is determined by

$$N = T_{reqd}/T_{maxj} \qquad j = 1, 2, 3 \tag{14}$$

where $T_{reqd}$ is the required thrust. Fuel flow is given by

$$\dot{W}_1 = k \cdot \dot{W}_1(N, M, h) \tag{15}$$

or

$$\dot{W}_2 = k \cdot \dot{W}_2(N, M, h) \tag{16}$$

or

$$\dot{W}_3 = k \cdot \dot{W}_3(M, h) \tag{17}$$

The parameter k is a scalar for adjusting fuel flow to meet various specification requirements. Vehicle thrust, T, is determined by

$$T = T_{reqd} \tag{18}$$

Within the program the simplified propulsion system input is scaled by appropriate factors to produce the following modified thrust and fuel flow data

$$(T)'_i = T_i/\sigma \quad ; \; i = 1, 2, 3 \tag{19}$$

$$(\dot{W})'_i = \dot{W}_i/(100 \times \Theta^{1.5}) \; ; \; i = 1, 2 \tag{20}$$

$$(\dot{W})'_3 = \dot{W}_3/\Theta^{1.5} \tag{21}$$

where $\sigma$ is the atmospheric density ratio and $\Theta$ is the atmospheric temperature ratio.

In the dry and wet options (i = 1 and 2, respectively), the power setting is specified as a percentage of maximum; hence, the factor of 100 in the scaling equations for fuel flow in the cases i = 1 and 2. Again, in the dry and wet options, three power setting options are possible. These correspond to

$$F_N = \left\{ \begin{array}{l} \text{Maximum available in system.....1} \\ \text{Required to equal drag.....2} \\ \text{Specified value of power setting....3} \end{array} \right\}$$

The corresponding fuel flows are determined from the power setting

$$PS = FN/(FN \text{ Maximum Available}) \qquad (22)$$

*It should be noted that power setting data is specified in the mission segment options of Section 6 and hence do not form part of the basic propulsion system input.*

### 2.2 Turbojet, Ramjet and/or Combined Engines with Inlet Precompression Effects (Combined Engine Option)

The turbojet, ramjet, and /or combined engine simulation option provided in NSEG by the ENGINS subroutine provides a more realistic engine simulation option for high speed flight than those described in Section 2.1 due to the following features:

1. Inlet flow field precompression effects due to airstream flow deflection are accounted for in thrust calculations.

2. A more accurate description of engine performance is provided by tabular engine data.

3. Turbojet only, ramjet only, or turbojet/ramjet combination engine options are provided; in-flight option selection as a function of Mach number can be employed.

4. Engine-related lift and drag forces are computed and accounted for in the net thrust and the desired vehicle lift.

5. High altitude and Mach number real gas atmospheric properties related to engine performance are described by tabular data.

The following sections provide an analytical description of the turbojet, ramjet and/or combined engine propulsion option and user-related information.

#### 2.2.1 Analytical Description

The basic assumption of two-dimensional inlet flow is employed in the turbojet, ramjet, and/or combined engine simulation subroutine. The geometry and various flow regions relevant to the simulation are shown in Figure (3). The computations performed are divided into seven main categories as follows.

1. Free stream properties at Station 0 which are a function of aircraft Mach number and altitude.

2. Flow field conditions at Station 1, aft of the wing shock.

3. Inlet computations which yield the turbojet inlet recovery ratio and ram drag.

4. Flow field conditions at Station 2, aft of the engine inlet wedge shock.

5. Turbojet thrust, airflow, and fuel flow computations, a function of flow field conditions at Stations 1 and 3 (at the turbojet compressor face) and throttle setting.

6. Ramjet thrust and fuel flow computations, a function of flow field conditions at Station 2 and $M_0$.

7. Spillage drag computations, if any, are performed either in the turbojet iteration loop for the turbojet alone engine option or in the ramjet iteration loop for the ramjet alone engine option, or the combined engine option, Figure 4.

Details of these computations are described in the following text.

### 2.2.2 Freestream Properties

For freestream conditions where $M \geq 3.5$ and altitude exceeds 19812 m (65000 ft), real gas freestream total pressure ($P_{t_0}$) and total temperature ($T_{t_0}$) values are determined by the two-dimensional table lookup subroutine DISCOT. Linear interpolation is utilized. Plots typical of these data appear in Figure (5). Freestream total pressure in p.s.f. is then given by

$$P_{t_0} = 2116.22 * P^* \qquad (P^* \text{in atmospheres}) \tag{23}$$

If the above Mach-altitude conditions are not satisfied, total temperature and total pressure values are computed by first determining freestream static conditions ($p_0, T_0$) from the 1962 Standard Atmosphere Subroutine ATMS62. Static enthalpy (H) and pressure ratio ($p_{r_0}$) are then determined from Table II, given the static temperature. Total enthalpy ($H_t$) can next be computed by the expression

$$H_T = H + (M_0 * a_0)^2/50073.2 \tag{24}$$

Given total enthalpy, the freestream total temperature and total pressure ratio ($P_{r_{t_0}}$) can be determined from Table II. Freestream total pressure is then given by

$$P_{t_0} = (P_{r_{t_0}}/P_{r_0}) * P_0 \tag{25}$$

### 2.2.3 Flowfield Conditions at Station 1

Given the freestream flowfield parameters at Station 0, their counterparts at Station 1 aft of the wing shock are determined by the two-dimensional isentropic shock relations (NASA Report 1135). These relationships are mechanized in the subroutine OBSHOK which performs oblique shock computations for wedge angles below the critical value and normal shock computations at higher wedge angle values.

### 2.2.4 Inlet and Ram Force Computations

Given flowfield parameters at Station 1 and the engine streamtube area, the ram drag is computed from the equation

$$\text{TURBOJET RAM FORCE} = \rho_1 * A_{T_J} * (M_1 * a_1)^2 + A_{T_J} (P_1 - P_0) \qquad (26)$$

where $A_{T_J}$ is the area of the stream tube of the airflow utilized by the turbojet. Ramjet ram forces are accounted for a priori in the ramjet specific impulse data. The ram force computed above, parallel to the vehicle wing under surface, is subsequently resolved into components in the lift and drag directions.

The engine capture ratio $(A_c/A_{FULL})$ is determined from Figure 6, Table III, given $M_1$. The air flow rate captured by the inlet then becomes

$$W_{A_c} = W_{A_{FULL}} * (A_c/A_{FULL}) = \rho_1 * A_{INLET} * M_1 * a_1 * (A_c/A_{FULL}) \qquad (27)$$

Capture ratio less than 1.0 indicates operation at a below design Mach number. As seen in Figure (3) the result of below design operation is that the wedge shock fails to intersect the inlet cowl resulting in inlet air spillage. This spillage produces forces (inlet spillage lift and drag) which are computed using a combination of continuity relationships and geometry as shown in Figure (4).

### 2.2.5 Flowfield Conditions at Station 2

Given the flowfield parameters at Station 1, conditions at Station 2 are computed using subroutine OBSHOK as in 2.2.3 above. That is the two-dimensional flow behind the precompression (wing) surface shock is turned again through the inlet wedge angle $(\delta_I)$.

### 2.2.6 Turbojet Airflow, Fuel Flow and Thrust Computations

For a base size turbojet, airflow and fuel flow requirements at full throttle are first determined via the one-dimensional table lookup routine FTLUP. The corresponding maximum thrust is determined via the two-dimensional table lookup routine DISCOT. The corrected airflow $(W\sqrt{\theta}/\delta)$ requirement is determined from Table V, given the total temperature at Station 3 $(T_{t_3})$. This value is then used to determine the turbojet airflow at any flight condition by the equation:

$$W_A = (W_A)_{corrected} * \delta/\sqrt{\theta} * F_{T_J} \quad (28)$$

where

$(W_A)_{corrected}$ = the base engine corrected airflow rate.

$\delta = P_{t_3}/2116.22$, ratio of compressor face total pressure to sea level static pressure. (29)

$\theta = T_{t_3}/518.67$, ratio of compressor face total temperature to sea level static temperature. (30)

$F_{T_J}$ = **the turbojet scaling factor obtained by specifying (1) desired net thrust at sea level standard conditions or (2) desired turbojet airflow at sea level standard conditions**

Note: It is assumed that $T_{t_3} = T_{t_2} = T_{t_1} = T_{t_0}$ (Figure 3).

The fuel flow rate to air flow ratio is determined from Figure 7, Table VII, given $T_{t_3}$. The maximum turbojet thrust to air flow rate is found from Table VI[3] using the two-dimensional table lookup routine DISCOT, given $T_{t_3}$ and the log to the base ten of the ratio of total pressure at Station 3 at the compressor face and a reference turbojet discharge region static pressure $P_N$ which may either be the underwing pressure or the freestream static pressure. The above pressure ratio is obtained by first determining $P_{t_3}/P_{t_1}$ from Table IV, given $M_1$, and multipyling by $P_{t_1}/P_N$.

The fuel flow rate, maximum thrust and specific fuel consumption are then computed as follows:

$$(W_f)_{MAX} = (W_A) * (W_f/W_A) \quad (31)$$

$$F_{MAX} = (F_G/W_A) * (W_A) \quad (32)$$

$$(SFC)_{MAX} = (W_f)_{MAX}/(F_N)_{MAX} \quad (33)$$

Where $(F_N)_{MAX}$ is the maximum net thrust of the turbojet given by the expression

$$(F_N)_{MAX} = F_{MAX} - \text{Ram Force} \quad (34)$$

Note that the specific fuel consumption given above has units of (Lb. Fuel/Sec)/Lb. Thrust. The non-standard time unit is employed to be compatible with subsequent weight computations in NSEG. The fuel/air ratio $W_F/W_A$ is obtained from Table VII, given $T_{t_3}$.

The program is constructed to allow thrust required in the flight direction to be determined either by a turbojet throttle setting input or a thrust required input. If the throttle setting option is exercised thrust required is computed as

$$F_R = T_J * F_N \tag{35}$$

where $T_J$ is the turbojet throttle setting input. If $F_R$ is input greater than the net thrust which the turbojet can provide in the combined engine mode, the excess thrust will be provided by the ramjet, if possible. Prior to entering the turbojet iteration loop the maximum turbojet net thrust is computed

$$(F_N)_{MAX} = F_{MAX} - \text{RAM DRAG} \tag{36}$$

and miscellaneous iteration parameters are initialized.

The purpose of the turbojet iteration loop is to provide the net thrust required, if possible, totally by throttling the turbojet. This procedure requires that spillage drag, a function of turbojet throttle setting, be accounted for in the net thrust, i.e.,

$$F_{T_J} = F_R = (F_{TOT})_{T_J} \cdot \cos\gamma - \text{RAM DRAG} - \text{SPILLAGE DRAG} \tag{37}$$

In the above expression $\gamma$ is the angle between the wing under surface and the freestream direction, RAM DRAG is the component of RAM FORCE in the freestream direction and SPILLAGE DRAG includes drag components due to inlet spillage and excess captured air spillage, if any.

The logic within this loop first tests the turbojet throttle setting. If this value is less than one, iteration commences. Otherwise, turbojet throttle setting and total thrust are adjusted to their maximum values and a check for the combined engine option is made. If the combined engine option is not requested, an optional message will indicate that the thrust requested is higher than that which can be provided. Within the iteration loop, throttled turbojet performance parameters are computed by first determining the throttled engine SFC ratio from Table VIII, given the throttled net thrust to maximum net thrust ratio. The throttled SFC, fuel flow rate, and airflow rate then become simply

$$SFC = (SFC)_{MAX} * SFC/(SFC)_{MAX} \quad (38)$$

$$(W_f)_{TJ} = SFC * (F_{TOT})_{TJ} \quad (39)$$

$$(W_A)_{TJ} = (W_f)_{TJ}/(W_f/W_A) \quad (40)$$

Since the throttled net thrust to maximum net thrust ratio required to compute turbojet airflow rate is a function of turbojet ram force which itself is a function of turbojet airflow rate, an iteration loop encompassing the above computations is required to ensure that the turbojet airflow rate used to compute the net thrust ratio is equal to that used to compute the ram drag.

If $W_A$ as computed above is less than the previously computed inlet captured airflow rate, the excess is spilled by the turbojet and results in either a spillage drag, a ramjet thrust, or both. If $W_A$ is greater than the inlet captured airflow rate, the excess is assumed to be available from suck-in doors.

If, (1) the turbojet throttle setting equals one and the combined engine option is selected or (2) a desired turbojet throttle setting has been specified by the subroutine input data the net turbojet thrust available in the freestream direction is computed by the expression:

$$F_{TJ} = (F_{TOT})_{TJ} * \cos\gamma - \text{RAM DRAG} - \text{INLET SPILLAGE DRAG} \quad (41)$$

and logic flow exits to ramjet calculations.

If the turbojet throttle setting is less than one, the spilled air lift and drag components due to spillage of excess captured air (engine spillage) are computed as shown in Figure 4. The available turbojet thrust is updated to account for engine spillage drag by the equation

$$F_{TJ} = (F_{TOT})_{TJ} * \cos\gamma - \text{RAM DRAG} - \text{INLET SPILLAGE DRAG} - \text{ENGINE SPILLAGE DRAG} \quad (42)$$

A maximum throttle setting check followed by a satisfactory thrust level check are performed; satisfaction of either results in a return to the calling routine. The iteration loop following no exit is a simple application of Newton's method which attempts to satisfy the required thrust level within one tenth of one per cent. A maximum of ten iterations is allowed to complete this requirement. The independent variable in this process is the total turbojet thrust. In the event convergence is not achieved in ten iterations, an error message is printed and a return to the calling program is executed with the engine parameters computed on the last iteration.

### 2.2.7 Ramjet Airflow, Fuel Flow, and Thrust Computations

The ramjet computation sequence is constructed similar to that for the turbojet. The maximum ramjet air flow rate to the full capture inlet air flow rate is computed from Table X given the total temperature at Station 2, $T_{t_2}$. The maximum ramjet air flow is then, simply,

$$(W_A)_{RJ\ MAX} = \frac{(W_A)_{MAX}}{(W_A)_{FULL}} * (W_A)_{FULL} \tag{43}$$

The ramjet actual fuel/air ratio divided by the stoichiometric fuel/air ratio and ramjet specific impulse are determined from Table IX as a function of freestream Mach number. Engine spillage drag, if any, ramjet and total fuel flow rates, air flow rates, and net available thrust levels are computed in the ramjet iteration loop via the equations:

$$(W_f)_{RJ} = \frac{(W_f/W_A)_{R.J.}}{(W_f/W_A)_{\text{Stoichiometric}}} * (W_A)_{RJ} * (W_f/W_A)_{\text{Stoichiometric}} \tag{44}$$

$$F_{RJ} = (W_f)_{RJ} * I_{SP} * \cos\gamma - \text{SPILLAGE DRAG} \tag{45}$$

$$(W_f)_{TOT} = (W_f)_{RJ} + (W_f)_{TJ} \tag{46}$$

$$(W_A)_{TOT} = (W_A)_{RJ} + (W_A)_{TJ} \tag{47}$$

$$F_{NET} = F_{RJ} + F_{TJ} \tag{48}$$

Where the ramjet air flow rate above is either due to the air flow spilled from the turbojet or the maximum ramjet air flow rate, which ever is less. In the latter case, the excess air is spilled at pressure $P_2$ and engine spillage forces are computed. The term SPILLAGE DRAG above consists of only engine spillage drag in the combined engine option but includes inlet spillage drag in the ramjet only option. The ramjet iteration loop again applies Newton's method to satisfy, if possible, the thrust level requested within .1 per cent using the ramjet air flow rate as the independent variable. If this condition cannot be satisfied, an appropriate message is printed and a return to the calling routine is executed with the engine parameters last computed.

## 3. VEHICLE AERODYNAMIC REPRESENTATION

All aerodynamic representations compute the vehicle drag given a flight condition and lift coefficient. Vehicle lift coefficient required is determined internally by NSEG on the basis of instantaneous flight conditions.

### 3.1 Clean Aircraft

Either of two aerodynamic representations may be employed for the clean aircraft as described below.

#### 3.1.1 General Form

The clean aircraft drag is computed in the form

$$C_D = C_{D_o} + C_{D_i} \tag{49}$$

where $C_{D_o}$ is the zero lift drag, and $C_{D_i}$ is the induced drag.

Both $C_{D_o}$ qnd $C_{D_i}$ may be computed by three component summation; that is,

$$C_{D_o} = C_{D_{o1}} + C_{D_{o2}} + C_{D_{o3}} \tag{50}$$

$$C_{D_i} = C_{D_{i1}} + C_{D_{i2}} + C_{D_{i3}} \tag{51}$$

In Equation (50) each of the three component zero lift drags must be of the form

$$C_{D_{oj}} = C_{D_{oj}}(h, M);\ j = 1, 2, 3 \tag{52}$$

Similarly, in Equation (51) each induced drag component must be of the form

$$C_{D_{ij}} = C_{D_{ij}}(C_L, M);\ j = 1, 2, 3 \tag{53}$$

#### 3.1.2 Polynomial Form

In this aerodynamic option the drag is computed in the component summation form

$$C_D = C_{D_1} + C_{D_2} + C_{D_3} \tag{54}$$

where

$$C_{D_j} = C_{D_{oj}} + k_{1_j} \cdot C_L{}^2 + k_{2_j}(C_L - C_{L_{MIN}})^2 + k_{3_j}C_L{}^3$$

$$j = 1, 2, 3 \tag{55}$$

and

$$C_{D_{oj}} = C_{D_{oj}}(M) \tag{56}$$

$$k1_j = K1_j(M) \tag{57}$$

$$k2_j = k2_j(M) \tag{58}$$

$$k3_j = k3_j(M) \tag{59}$$

$$C_{L_{MIN}} = C_{L_{MIN}}(M), \text{ the minimum drag lift coefficient} \tag{60}$$

## 3.2 Store and Pylon Drag

Store and pylon drag is computed in the form

$$C_{D_S} = C_{D_1} + C_{D_2} + C_{D_3} \tag{61}$$

where

$$C_{D_j} = C_{D_{S_j}} \cdot N_{S_j} + C_{D_{SP_j}} \cdot N_{SP_j} \qquad j = 1, 2, 3 \tag{62}$$

In Equation (7.2.25) the drag of a single type j store pair is

$$C_{D_{S_j}} = C_{D_{S_j}}(M) \tag{63}$$

The number of type j store pairs is $N_{S_j}$. The drag of a single type j store pylon pair is

$$C_{D_{SP_j}} = C_{D_{SP_j}}(M) \tag{64}$$

The number of type j store pylon pairs is $N_{SP_j}$

## 3.3 Tank and Pylon Drag

Tank and pylon drag is computed in the form

$$C_{D_T} = C_{D_1} + C_{D_2} + C_{D_3} \tag{65}$$

where

$$C_{D_j} = C_{D_{T_j}} \cdot N_{T_j} + C_{D_{TP_j}} \cdot N_{TP_j} \qquad j = 1, 2, 3 \tag{66}$$

In Equation (7.2.29) the drag of a single type j tank pair is

$$C_{D_{T_j}} = C_{D_{T_j}}(M) \tag{67}$$

The number of type j tank pairs is $N_{T_j}$. The drag of a single type j tank pylon pair is

$$C_{DTP_j} = C_{D_{TP_j}}(M) \tag{68}$$

The number of type j tank pylon pairs is $N_{TP_j}$.

### 3.4 Centrifugal Lift

Centrifugal lift accounts for the earth's curvature. In flight at constant altitude about a circular earth a vehicle is effectively falling to follow the earth's surface. In consequence the full vehicle weight is not supported during constant altitude cruise. It can be shown that the relieving centrifugal lift term is given by

$$C_{L_{cent}} = \frac{W(V \cos \gamma)^2}{qS} \left[ \frac{R_e + h}{G_o R_e^2} \right]$$

## 4. VEHICLE MASS REPRESENTATION

### 4.1 Overall Weight Empty

The vehicle overall weight empty is given by the following equation:

$$W_{OWE} = W_{BARE} + \sum_{i=1}^{3}(N_{S_i} \cdot W_{S_i})_{fixed} + \sum_{i=1}^{3}(N_{SP_i} \cdot W_{SP_i})_{fixed}$$

$$+ \sum_{i=1}^{3}(N_{T_i} \cdot W_{T_i})_{fixed} + \sum_{i=1}^{3}(N_{TP_i} \cdot W_{TP_i})_{fixed} \qquad (69)$$

where

$W_{OWE}$ = overall weight empty

$W_{BARE}$ = bare weight without stores, tanks, or pylons

$N_{S_i}$ = number of store pairs type i

$W_{S_i}$ = weight of one store pair type i

$N_{SP_i}$ = number of store pylon pairs type i

$W_{SP_i}$ = weight of one store pylon pair type i

$N_{T_i}$ = number of tank pairs type i

$W_{T_i}$ = weight of one tank pair type i

$N_{TP_i}$ = number of tank pylon pairs type i

$W_{TP_i}$ = weight of a tank pylon pair type i

The suffix fixed indicates that only fixed tanks, stores or pylons which are not included in the payload must be included in the summations.

## 4.2 Fuel Load

The total vehicle fuel load is given by

$$W_{FUEL} = W_{FINT} + \sum_{i=1}^{3}(N_{T_i} \cdot W_{FT_i})_{usable} \qquad (70)$$

where

$W_{FUEL}$ = total useable fuel weight

$W_{FINT}$ = weight of internal fuel

$N_{T_i}$ = number of tank pairs type i

$W_{FT_i}$ = weight of fuel in one tank pair type i

The suffix usable indicates that the summation only extends over tank pairs which are not included in the payload.

The total non-payload fuel on board at mission initiation is given by

$$W_{FT_o} = W_{F_{INT}} + \sum_{i=1}^{3} (N_{T_i} \cdot W_{FT_i})_{NPL} \tag{71}$$

where

$W_{FT_o}$ = initial fuel load

$W_{F_{INT}}$ = initial internal fuel load

$N_{T_i}$ = number of tank pairs type i

$W_{FT_i}$ = weight of fuel in one tank pair type i

and the suffix NPL indicates the summation extends only over tanks which are not assigned to payload. It should be noted that the total fuel is specified directly by data input, and the internal fuel load is a computed quantity.

## 4.3 Payload

The total vehicle payload on board at mission initiation is given by

$$W_{PL} = W_{PL_{int}} + \sum_{i=1}^{3} (N_{S_i} \cdot W_{S_i})_{drop} + \sum_{i=1}^{3} (N_{SP_i} \cdot W_{SP_i})_{drop}$$

$$+ \sum_{i=1}^{3} (N_{T_i} \cdot W_{T_i})_{drop} + \sum_{i=1}^{3} (N_{ST_i} \cdot W_{TP_i})_{drop} \tag{72}$$

where

$W_{PL}$ = total payload

$W_{PL_{int}}$ = total internal payload

and the remaining quantities in Equation (72) are defined in Section 4.1.

## 5. PLANETARY REPRESENTATION

A flat earth planetary model is employed. The gravitational force is a simple inverse square field. A layered atmosphere provides the following options:

1. Tabular 1962 U. S. Standard Atmosphere
2. Analytic 1962 U. S. Standard Atmosphere
3. 1963 Patrick Air Force Base Atmosphere
4. 1959 U. S. Standard Atmosphere
5. January 1966 NASA Atmosphere, 30° North
6. July 1966, NASA Atmosphere, 30° North
7. Arbitrary Atmosphere Generated from Temperature and/or Pressure Variation with Altitude

The NSEG program basically computes a planar flight path. However, time to turn calculations are available; hence, a three-dimensional path can be analyzed by "folding" the path into a plane, Figure 8.

## 6. FLIGHT PATH ANALYSIS

Flight path analyses for take-off, climb, cruise, descent, and landing are included in NSEG. The analyses are all based on relatively rapid approximate methods. Each flight path analysis model employed is described below.

### 6.1 Take-Off

The take-off analysis performs the transfer

$$\{X\}_{TO} \rightarrow \{X\}_{50} \tag{73}$$

where the suffix TO indicates state at beginning of take-off, and the suffix 50 indicates state at the 15.24 m (50 ft.) obstacle.

The take-off model was originally developed by Mr. Louis J. Williams of NASA's Advanced Concepts and Missions Division, OART, Ames Research Center. The program provides:

1. Simplified high lift aerodynamics based on the USAF DATCOM
2. A ground roll analysis
3. Rotation logic
4. Climb out to clear a 15.24 m (50 ft.) obstacle

The take-off analysis is also available as a stand-alone code, program TOLAND.

### 6.1.1 Take-Off High Lift Aerodynamics

The take-off model uses a self-contained aerodynamics package based primarily on the DATCOM methods. Angle of attack in the ground run and rotation maneuvers is determined from the vehicle geometry. In the *ground roll*

$$\alpha_G = \alpha_{BG} + \alpha_{WB} \tag{74}$$

where
$\alpha_G$ = wing incidence in ground roll
$\alpha_{BG}$= body incidence in ground roll
$\alpha_{WB}$= wing incidence relative to body

In the rotated attitude

$$\alpha_R = \alpha_{B_{MAX}} - 1.0 + \alpha_{WB} \tag{75}$$

The additional symbols are

$\alpha_R$ = wing incidence following rotation
$\alpha_{B_{MAX}}$ = maximum body rotation, usually determined by the tail dragging condition

#### 6.1.1.1 Take-Off Lift and Drag

##### 6.1.1.1(a) Maximum Lift and Drag

The wing maximum lift coefficient is given by

$$C_{L_{MAX}} = (C_{L_{MAX}})_{BASE} + \Delta C_{L_{MAX}} + \Delta C_{L_{FLAP}} \tag{76}$$

with a corresponding angle of attack

$$\alpha' = (\alpha C_{L_{MAX}})_{BASE} \tag{77}$$

During take-off the maximum angle of attack, $\alpha_{MAX}$, is limited to

$$\alpha_{MAX} = 0.8 \cdot \alpha' \tag{78}$$

In these two expressions

$C_{L_{MAX}}$ =wing lift coefficient at the first peak, Figure 9

$(C_{L_{MAX}})_{BASE}$ =basic wing maximum lift coefficient

$\Delta C_{L_{MAX}}$ =maximum lift coefficient increment due to taper and sweep

$\Delta C_{L_{FLAP}}$ =maximum lift coefficient increment from flap deflection

$(\alpha C_{L_{MAX}})_{BASE}$ =basic wing angle of attack at maximum lift coefficient based on linear $C_{L_\alpha}$ term. Nonlinear $\alpha$ increment is ignored.

The high lift aerodynamic model is a simplified DATCOM method for subsonic low aspect ratio, untwisted, symmetric section wings. Due to the low speeds encountered in take-off and landing, the DATCOM method is modified by the approximation

$$\beta = \sqrt{1-M^2} = 1.0 \tag{79}$$

Clean wing contributions to Equations (76) and (78) are obtained from Figures 10 and 11. Figure 10 provides $(C_{L_{MAX}})_{BASE}$; Figure 11 gives $\Delta C_{L_{MAX}}$. The wing taper ratio correction factors C1 and C2 of Figures 10 and 11 are obtained from Figure 12. In Figure 10, the take-off model is limited to the lowest curve, and the curve for $M \leq 0.2$ is used in Figure 11. Angle of attack at maximum lift coefficient is obtained from Figure 13.

Flap maximum lift coefficient increment is based on the expression

$$\Delta C_{L_{FLAP}} = 10.95 (C_{L_A})_{BASE} \left[1.5 \left(\frac{B_F}{B_{WE}}\right) - 0.5 \left(\frac{B_F}{B_{WE}}\right)^2\right] \times \left(\frac{\bar{C}_F}{\bar{C}_{WE}}\right)^{1/2} [.0625 \int_F - .000472 \int_F^2] \tag{80}$$

where

$(C_{L_A})_{BASE}$ = linear lift coefficient slope/degrees

$B_F$ = flap span

$B_{WE}$ = exposed wing span

$\bar{C}_F$ = average flap chord

$\bar{C}_{WE}$ = average exposed wing chord

$\int_F$ = flap deflection

6.1.1.1(b) Ground Roll Lift and Drag

During the ground roll, the lift coefficient is determined by

$$C_{L_G} = 57.29\, C_{L_\alpha} \cdot \sin(\alpha_G) \cos^2(\alpha_G) + \left[\frac{C_{L_{MAX}}}{\cos(\alpha_{MAX})} - \frac{57.29}{2} C_{L_\alpha} \sin(\alpha_{MAX})\right]$$

$$= F(\alpha_G) \quad \sin^2(\alpha_G) \cos(\alpha_G)/\sin^2(\alpha_{MAX}) \tag{81}$$

where $C_{L_\alpha}$ is the linear lift curve slope. The corresponding ground roll drag is taken as

$$C_{D_G} = C_{D_o} + k \cdot C_{L_G}[C_{L_G} - C_{L_o} - \Delta C_{L_{FLAP}}] + C_{D_{LG}} \tag{82}$$

where

$C_{D_o}$ = zero lift drag coefficient
k = induced drag factor
$C_{L_o}$ = lift coefficient at zero wing incidence
$C_{D_{LG}}$ = landing gear drag coefficient

6.1.1.(c) Rotation Lift and Drag

The lift coefficient after rotation, $C_{L_R}$, is given by Equation (81) with $\alpha_R$ replacing $\alpha_G$; that is,

$$C_{L_R} = F(\alpha_G) \tag{83}$$

The lift coefficient is subject to the condition that

$$C_{L_R} \leq (C_{L_{MAX}})/(1.1)^2 \tag{84}$$

This inequality constraint is imposed to prevent buffet or pitch-up problems.

The drag coefficient after rotation is given by

$$C_{D_R} = C_{D_o} + kC_{L_R}[C_{L_R} - C_{L_o} - \Delta C_{L_{FLAP}}] + C_{D_{LG}} \tag{85}$$

6.1.1.1(d) Lift and Drag at 15.24 m (50 feet) Obstacle

The lift coefficient at a 15.24 m (50 feet) obstacle is based on the rotation lift coefficient.

$$C_{L_{50}} = C_{L_R}/(1.1)^2 \tag{86}$$

The corresponding drag is given by

$$C_{D_{50}} = C_{D_o} + k \cdot C_{L_{50}}[C_{L_{50}} - C_{L_o} - \Delta C_{L_{FLAP}}] + C_{D_{LG}} \tag{87}$$

## 6.1.2 Ground Roll and Rotation

The ground roll distance, $X_G$, is based on the expression

$$X_G = \frac{13.07(\frac{W_{TO}}{S.C_{L_R}})}{\frac{F_{TO}}{W_{TO}} - \mu_G - \frac{1}{2}(\frac{C_{D_{GR}}}{C_{L_R}})} \tag{88}$$

where

$$C_{D_{GR}} = \frac{1}{2}(C_{D_G} + C_{D_R}) \tag{89}$$

and
$F_{TO}$ = take-off thrust

$W_{TO}$ = take-off weight

$\mu_G$ = vehicle rolling friction coefficient

Time to reach the rotation point is given by

$$T_G = 1.1842\ X_G/V_R \tag{90}$$

where the velocity at rotation, $V_R$, is given by

$$V_R = 17.16\sqrt{\frac{W_{TO}}{SC_{L_R}}} \tag{91}$$

Rotation is assumed to occur instantaneously.

### 6.1.3 Flight to Clear 15.24 m (50 feet) Obstacle

The average drag coefficient between rotation and 15.24 m (50 feet) obstacle clearance points is assumed to be

$$C_{D_{R50}} = \frac{1}{2}(C_{D_R} + C_{D_{50}}) \tag{92}$$

The distance covered in clearing the obstacle is given by

$$X_{50} = \frac{50.0+2.745\left(\frac{W_{TO}}{S\cdot C_{L_R}}\right)}{\left(\frac{F_{TO}}{W_{TO}}\right) - 1.105\left(\frac{C_{D_{R50}}}{C_{L_R}}\right)} \tag{93}$$

Time to clear the obstacle after rotation is

$$T_{50} = X_{50}/(1.6889 \times V_R) \tag{94}$$

**Thus, total distance for take-off over** 15.24 m (50 feet) obstacle is

$$X_{TO} = X_G + X_{50} \tag{95}$$

**The elapsed time is**

$$T_{TO} = T_G + T_{50} \tag{96}$$

**Total fuel used is**

$$W_{F_{TO}} = F_{TO} \cdot T_{TO}/(I_{SP_{TO}}) \tag{97}$$

At the 15.24 m (50 feet) obstacle the flight path angle is obtained from

$$\sin(\gamma_{50}) = \frac{F_{TO}}{W_{50}} - \frac{C_{D50}}{C_{L50}} \tag{98}$$

where

$$W_{50} = W_{TO} - W_{F_{TO}} \tag{99}$$

The corresponding rate of climb is given by

$$RC_{50} = 1.6889\ V_{50}\ \sin(\gamma_{50}) \tag{100}$$

## 6.2 Landing High Lift Aerodynamics

The landing analysis closely follows the take-off analysis but in reverse sequence starting from the 15.24 m (50 feet) obstacle. The angle of attack at touchdown is

$$\alpha_{TD} = \alpha_{BTD} - 1.0 + \alpha_{WB} \tag{101}$$

and in the subsequent ground roll

$$\alpha_{LR} = \alpha_{BLR} + \alpha_{WB} \tag{102}$$

where

$\alpha_{TD}$ = wing incidence at touch down

$\alpha_{BTD}$ = body incidence at touch down

$\alpha_{LR}$ = wing incidence during landing ground roll

$\alpha_{BLR}$ = body incidence in landing ground roll

### 6.2.1 Landing Lift and Drag

The wing maximum lift coefficient during landing and the corresponding angle of attack are given by Equations (76) to (78). Flap incremental lift is given by Equation (80). It should be noted that the landing configuration parameters such as flap angle and permissible body angle of attack will normally differ significantly between the take-off and landing configurations. At the 15.24 m (50 feet) obstacle, configuration lift is assumed to be

$$C_{L_{L50}} = C_{L_{TD}}/(1.1)^2 \tag{103}$$

At touchdown, $C_{L_{TD}}$, is based on Equation (80) using $\alpha_{TD}$; that is

$$C_{L_{TD}} = F(\alpha_{TD}) + \Delta C_{L_{FLAP}} \tag{104}$$

where $\Delta C_{L_{FLAP}}$ is given by Equation (80) using the landing flap setting. The inequality

$$C_{L_{TD}} < C_{L_{MAX}}/(1.1)^2 \tag{105}$$

is used.

Similarly, during the subsequent landing ground roll,

$$C_{L_{LR}} = F(\alpha_{LR}) \tag{106}$$

Drag coefficient at the 15.24 m (50 feet) obstacle, $C_{DL50}$, is given by Equation (82) using appropriate landing coefficients. Drag at touchdown, $C_{D_{TD}}$, is given by Equation (7.1.8) using touchdown coefficients. Drag during the landing ground roll is given by

$$C_{D_{LR}} = C_{D_o} + k \cdot C_{L_{LR}}(C_{L_{LR}} - C_{L_o}) + C_{D_{LG}} + C_{D_{CHUT}} \tag{107}$$

where

$C_{D_{CHUT}}$ = landing parachute drag

All other symbols are defined in Section 6.1.1.

### 6.2.2 Flight from 15.24 m (50 feet) Obstacle to Touchdown

Velocity at touchdown is assumed to be

$$V_{TD} = 17.16 \sqrt{\frac{W_L}{S \cdot C_{L_{TD}}}} \tag{108}$$

The ground distance covered from 15.24 m (50 feet) obstacle to touchdown is

$$X_{L50} = \frac{50.0 + 2.745\left(\frac{W_L}{S \cdot C_{L_{TD}}}\right)}{1.105\left(\frac{C_{D_{TD50}}}{C_{L_{TD}}}\right) - \left(\frac{F_L}{W_L}\right)} \tag{109}$$

where

$X_{L50}$ = flight distance from 15.24 m (50 feet) obstacle to touchdown

$W_L$ = landing weight

$C_{D_{TD50}}$ = $\frac{1}{2}(C_{D_{50}} + C_{D_{TD}})$, the average drag coefficient

$F_L$ = approach thrust

**Rate of sink at the** 15.24 m (50 feet) obstacle is

$$RS_{50} = 1.69\ V_{50}\left[\left(\frac{C_{D_{L50}}}{C_{L_{L50}}}\right) - \left(\frac{F_{L50}}{W_L}\right)\right] \tag{110}$$

**Flight path angle at the** 15.24 m (50 feet) is given by

$$\sin(\gamma_{L50}) = \left(\frac{C_{D_{L50}}}{C_{L_{L50}}}\right) - \left(\frac{F_{L50}}{W_L}\right) \tag{111}$$

**The ground roll distance is given by**

$$X_{GL} = \frac{13.07\left(\frac{W_L}{S \cdot C_{L_{TD}}}\right)}{\mu + \frac{1}{2}(C_{D_{LG}} - \mu \cdot C_{L_{LR}})/C_{L_{TD}}} \tag{112}$$

**Total landing distance is**

$$X_L = X_{L50} + X_{GL} \tag{113}$$

## 6.3 Alternative High Lift Aerodynamics

Where detailed high lift aerodynamic values are known the DATCOM calculations may be bypassed. In this case the values of $C_{L_\alpha}$, $C_{L_{MAX}}$ and $\alpha_{MAX}$ (CLATØT, CLMXTØ, ALMXTØ) are specified directly in program input.

### 6.3.1 Acceleration at Constant Altitude

The level flight acceleration segment performs the operation

$$\{X\}_2 = \{X\}_1 + \int_{X_1}^{X_2} \dot{\{X\}} dM \simeq \{X_1\} + \sum_i \{\Delta X\}_i \tag{114}$$

where $\{\Delta X\}_i$ is the state change in accelerating from M to M + ΔM.

Given $\{X\}_i = \{V, h, \gamma, W, R, t\}_i$, $T_i$ and $D_i$, then the velocity change is

$$V = a_s\ \Delta M \tag{115}$$

where $a_s$ is the speed of sound at the acceleration altitude and

$$\dot{V}_i = g_o \left[\frac{T-D}{W}\right]_i \tag{116}$$

The approximate time to accelerate from $M_i$ to $M_i + \Delta M$ is

$$\Delta t' = \Delta V/\dot{V}_i \tag{117}$$

The corresponding approximate weight change is

$$\Delta W' = \dot{W}_i \, \Delta t' \tag{118}$$

and

$$W_{i+1} = W_i - \Delta W' \tag{119}$$

and to the first order

$$\dot{V}_{i+1} = g_o \left[\frac{T-D}{W}\right]_{i+1} \tag{120}$$

$W_{i+1}$ can be obtained at the new Mach number. The mean acceleration is now

$$\bar{\dot{V}} = \frac{1}{2}(\dot{V}_i + \dot{V}_{i+1}) \tag{121}$$

The revised time to accelerate is

$$\Delta t = \Delta V/\bar{\dot{V}} \tag{122}$$

which gives a weight change of

$$\Delta W = \frac{1}{2}(\dot{W}_i + \dot{W}_{i+1})\Delta t \tag{123}$$

and a range increment

$$\Delta R = \frac{1}{2}(V_i + V_{i+1})\Delta t \tag{124}$$

The state incremental vector $\{\Delta X\}_i$ is therefore given by

$$\begin{bmatrix} \Delta V \\ \Delta h \\ \Delta \gamma \\ \Delta R \\ \Delta W \\ \Delta t \end{bmatrix} = \begin{bmatrix} a_s \Delta M \\ 0 \\ 0 \\ \frac{1}{2}(V_i + V_{i+1})\Delta t \\ \frac{1}{2}(\dot{W}_i + \dot{W}_{i+1})\Delta t \\ \frac{2\Delta V}{(\dot{V}_i + \dot{V}_{i+1})} \end{bmatrix} \tag{125}$$

## 6.4 Accelerating Climbs

All accelerating climb paths are formed by a sequence of elemental straight line arcs in the Mach-altitude plane. On any arc the vehicle flies from $(M_i, h_i)$ to $(M_{i+1}, h_{i+1})$. Since the vehicle is climbing

$$h_{i+1} > h_i \tag{126}$$

The typical arc for a climb path is shown below. The Mach-altitude plane

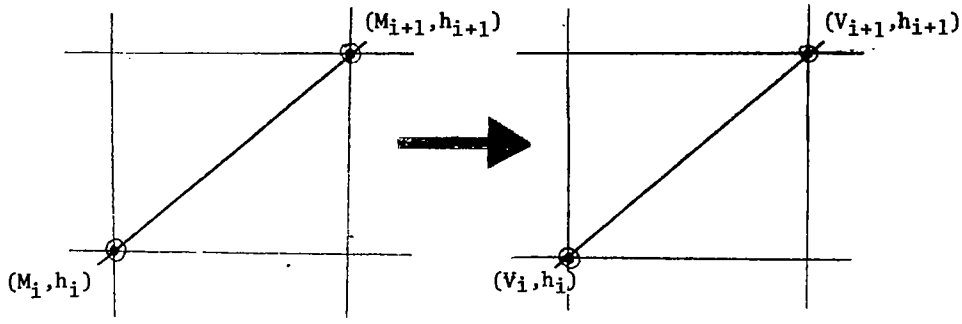


can be transformed into the velocity-altitude plane as follows:

$$V = V(h, M) \tag{127}$$

so that

$$\Delta V = \frac{\partial V}{\partial h} \cdot \delta h + \frac{\partial V}{\partial M} \delta M \tag{128}$$

or

$$\frac{dV}{dh} = \frac{\partial V}{\partial h} + \frac{\partial V}{\partial M} \cdot \frac{\partial M}{\partial h} \tag{129}$$

$$\frac{\partial V}{\partial h} + a \frac{dM}{dh} \tag{130}$$

where a is the local speed of sound

$$V = aM \tag{131}$$

Now $\partial V/\partial h$ is the change in velocity with altitude at constant Mach number, and from Equation (131) with M constant

$$\frac{\partial V}{\partial h} = M \frac{\partial a}{\partial h}$$

$$= M \frac{\partial a}{\partial T_R} \cdot \frac{dT_R}{dh} \tag{132}$$

where $T_R$ is temperature ratio, $T/T_{SL}$, so that

$$\frac{\partial V}{\partial h} = \left(\frac{V}{a}\right) \cdot \frac{\partial a}{\partial T_R} \cdot \frac{dT_R}{dh} \tag{133}$$

and from the atmospheric model

$$a = 1116.45(T_R)^{1/2} \tag{134}$$

$$\frac{\partial a}{\partial T_R} = \frac{a}{2\,T_R} \tag{135}$$

Substituting into Equation (133)

$$\frac{\partial V}{\partial h} = \frac{V}{2\,T_R} \cdot \frac{dT_R}{dh} \tag{136}$$

Substituting Equation (136) into Equation (130)

$$\frac{dV}{dh} = \frac{V}{2T_R} \cdot \frac{dT_R}{dh} + a\,\frac{dM}{dh} \tag{137}$$

Equation (137) is used to define the required variation of velocity with altitude over an elemental climbing arc.

Now the rate of climb is

$$\frac{dh}{dt} = RC \tag{138}$$

or

$$\frac{dh}{RC} = dt \tag{139}$$

*Assuming rate of climb varies linearly with altitude* in the elemental arc

$$RC = a + bh \tag{140}$$

Substituting into Equation (139) and integrating

$$\int_{h_1}^{h_2} \frac{dh}{(a+bh)} = \int_{t_1}^{t_2} dt \tag{141}$$

or

$$t_{i+1} - t_i = \left[\frac{h_{i+1}-h_i}{RC_{i+1}-RC_i}\right] \log\left(\frac{RC_{i+1}}{RC_i}\right) \tag{142}$$

where

$$a = RC_i \tag{143}$$

$$b = \frac{RC_{i+1} - RC_i}{h_{i+1} - h_i} \tag{144}$$

The vehicle rate of climb is computed under the assumption that thrust is aligned along the velocity vector as shown below.

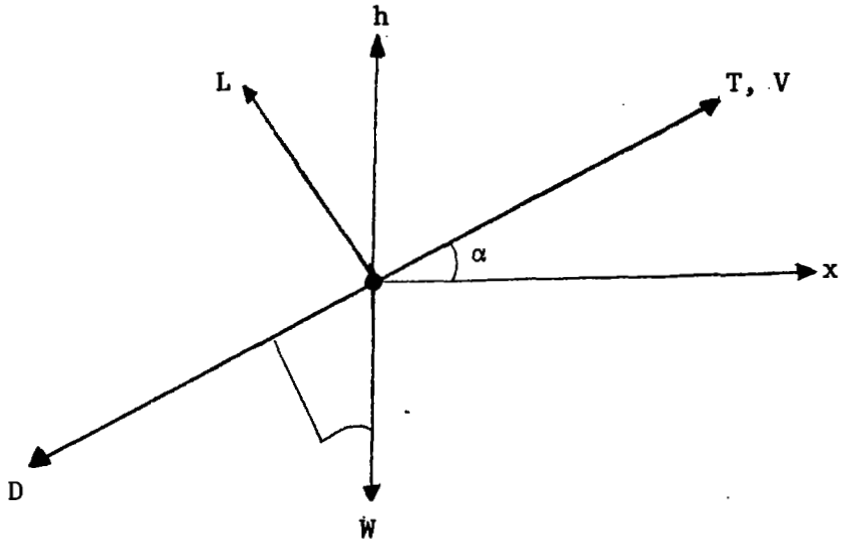


Now

$$m\dot{V} = (T - D) - W \sin\gamma \tag{145}$$

but

$$m\dot{V} = m \frac{dV}{dh} \cdot \frac{dh}{dt} = \frac{W}{g} \frac{dV}{dh} \cdot V \sin\gamma \tag{146}$$

Combining Equations (145) and (146)

$$\sin\gamma = \frac{T-D}{W\left[\frac{V}{g}\frac{dV}{dh} + 1.0\right]} \tag{147}$$

and

$$\cos\gamma = \sqrt{1-\sin^2\gamma} \tag{148}$$

so that

$$RC = V \sin\gamma = \left[\frac{(T-D)V}{W}\right] \Big/ \left[\frac{V}{g}\frac{dV}{dh} + 1.0\right] \tag{149}$$

Equation (149) can be evaluated at each end of the elemental arc to obtain $RC_{i+1}$ and $RC_i$. Hence, $\Delta t$, the time to traverse the elemental arc, is given by Equation (143). Similarly, the flight path angle at each end of the arc can be obtained from Equation (147). It should be noted that if $\sin\gamma$, Equation (148), is greater than 1.0, the approximate climb analysis is invalid. If this condition occurs, the thrust is reduced to produce a climb along the elemental arc at 89.5 degrees.

Summarizing, the state incremental vector for an accelerating climb is given by

$$\begin{bmatrix} \Delta V \\ \Delta h \\ \Delta \gamma \\ \Delta R \\ \Delta W \\ \Delta t \end{bmatrix} = \begin{bmatrix} V_{i+1} - V_i \\ h_{i+1} - h_i \\ \gamma_{i+1} - \gamma_i \\ \frac{1}{2}[V_{i+1} \cos\gamma_{i+1} + V_i \cos\gamma_i] \\ \frac{1}{2}[\dot{W}_{i+1} + \dot{W}_i]\Delta t \\ \frac{h_{i+1}-h_i}{RC_{i+1}-RC_i} \log\left[\frac{RC_{i+1}}{RC_i}\right] \end{bmatrix} \qquad (150)$$

### 6.4.1 Cruise Flight

Cruise flight performance is computed by the Breguet equation. With constant velocity the distance travelled in time $\Delta t$ is

$$\Delta R = V \cdot \Delta t \qquad (151)$$

Now

$$SFC = \frac{\dot{W}}{T} \qquad (152)$$

so that

$$\Delta t = \frac{\Delta W}{(SFC)\cdot T} \qquad (153)$$

Substituting in Equation (7.2.82)

$$\Delta R = \frac{V}{(SFC)\cdot T} \cdot \Delta W \qquad (154)$$

In cruise flight

$$\frac{L}{D} \simeq \frac{W}{T} \qquad (155)$$

and

$$\Delta R = \frac{V}{SFC}\left(\frac{L}{D}\right)\frac{\Delta W}{W} \tag{156}$$

On integrating

$$R_{i+1} - R_i = \frac{V}{SFC}\left(\frac{L}{D}\right)\log\left(\frac{W_{i+1}}{W_i}\right) = (RF)\log\left(\frac{W_{i+1}}{W_i}\right) \tag{157}$$

Where the range factor RF is usually a slowly changing function of weight. NSEG uses the inverse relationship to compute the weight change given a range increment

$$W_{i+1} = W_i e^{\left[\frac{R_{i+1}-R_i}{RF}\right]} = W_i e^{\left[\frac{(R_{i+1}-R_i)\cdot(SFC)}{V(L/D)}\right]} \tag{158}$$

Alternatively, the program can be used with a time increment $\Delta t$ by using the relationship

$$W_{i+1} = W_i e^{\left[\frac{\Delta t \cdot SFC}{(L/D)}\right]} \tag{159}$$

Several cruise modes are contained in the program including

1. Constant altitude, constant Mach number cruise
2. Constant altitude, constant $C_L$ cruise
3. Constant Mach number, constant $C_L$

Each of the three cruise modes may be performed in the manner

1. From $R_i$ to $R_{i+1} = \Delta R_i$
2. From $T_i$ to $T_{i+1} = \Delta T_i$
3. From $W_i$ to $W_{i+1} = \Delta W_i$

A cruise flight is computed by summing over $N_i$ steps. Thus,

$$\Delta R_{cruise} = \sum_i \Delta R_i$$

$$\Delta T_{cruise} = \sum_i \Delta T_i$$

or

$$\Delta W_{cruise} = \sum_i \Delta W_i$$

In all cases the total state increments are summed in the manner

$$\{\Delta X\}_{cruise} = \sum_i \{\Delta X\}_i \tag{160}$$

A mean range factor is used in all cruise calculations. The mean range factor, $(RC_i)$, in each elemental arc bounded by $\{X\}_i$ and $\{X\}_{i+1}$ is determined by an appropriate weighting of the range factors $RC_i$ and $RC_{i+1}$ which bound the arc.

## 6.5 Descent

The climb analysis of Section 6.4 is also used for the descent analysis. If the size of the flight path angle becomes too small ($\sin\gamma < -1$), the engine is throttled back to maintain a realistic flight path approximation.

## 6.6 Level Flight Acceleration

The approximate time to accelerate from $M_i$ to $M_{i+1}$ in level flight is

$$\Delta t_i' = a_s(M_{i+1} - M_i)/\dot{V}_i \tag{161}$$

with a corresponding weight change

$$\Delta W' = \dot{W}_i \, \Delta t' \tag{162}$$

so that

$$W_{i+1}' = W_i - \dot{W}_i \, \Delta t' \tag{163}$$

Therefore, to the first order

$$\dot{V}_{i+1} = g_o \left[\frac{T-D}{W}\right] \tag{164}$$

The fuel flow at this point, $\dot{W}_{i+1}$, can be obtained from the vehicle aerodynamic and propulsion representation.

$$\bar{\dot{V}}_i = \frac{1}{2}(\dot{V}_i + \dot{V}_{i+1}) \tag{165}$$

and an improved estimate of the time to accelerate from $M_i$ to $M_{i+1}$ is

$$\Delta t_i = a_s(M_{i+1} - M_i)/\bar{\dot{V}}_i \tag{166}$$

This gives an improved estimate of the weight change

$$\Delta W_i = \frac{1}{2}(\dot{W}_i + \dot{W}_{i+1})\ \Delta t_i \tag{167}$$

and the corresponding range change

$$\Delta R_i = \frac{1}{2}(V_i + V_{i+1})\ \Delta t_i \tag{168}$$

Summarizing, the level acceleration state increment is

$$\begin{bmatrix} \Delta h \\ \Delta V \\ \Delta \gamma \\ \delta W \\ \delta R \\ \Delta t_i \end{bmatrix} = \begin{bmatrix} 0.0 \\ a_s(M_{i+1} - M_i) \\ 0.0 \\ \frac{1}{2}(\dot{W}_i + \dot{W}_{i+1})\ \Delta t_i \\ \frac{a_s}{2}(M_{i+1} + M_i)\ \Delta t_i \\ \frac{a_s}{\partial g_o}(M_{i+1} - M_i)/[(\frac{T-D}{W})_i + (\frac{T-D}{W})_{i+1}] \end{bmatrix} \tag{169}$$

# 7. MISSION SEGMENTS

The state incremental methods of Section 6 are used to create a variety of optional mission segments in NSEG. Each available mission segment option is briefly described below. All mission climbs, cruises, accelerations, and decelerations may be performed in forward or reverse direction. Each mission segment described below is performed as a distinct option in NSEG. There is some degree of overlapping capability in the available mission options. The mission option within NSEG is indicated for each mission segment for reference purposes.

## 7.1 Generalized Climb or Descent (Mission Option 1)

The generalized climb descent option incorporates several alternative flight path estimation methods. These methods include:

Linear M-h path

Constant dynamic pressure path

Approximate optimal paths

Each of the available paths is described below.

### 7.1.1 Linear Climb

This option climbs linearly from $(M_i, h_i)$ to $(M_2, h_2)$ using a specified number of linear climb steps from $(M_i, h_i)$ to $(M_{i+1}, h_{i+1})$. The path is illustrated in Figure 14.

### 7.1.2 Climb at Specified Dynamic Pressure

This option climbs along a specified dynamic pressure line from $(M_1\ h_1)$ to $(M_2\ h_2)$ with appropriate terminal maneuvers. Along the constant dynamic pressure line a specified number of linear Mach-altitude segments are flown. Appropriate initial and final maneuvers are used when $(M_1\ h_1)$ or $(M_2\ h_2)$ do not lie on the specified dynamic pressure line. The user may specify a climb at the terminal end point dynamic pressure. In this case, the final maneuver is not required. This path is illustrated in Figure 15.

### 7.1.3 Rutowski Climb

The Rutowski climb, Reference 1 flies from $(M_1\ h_1)$ to $(M_2\ h_2)$ along the path which must rapidly build up specific energy. If either of the points $(M_1\ h_1)$ and $(M_2\ h_2)$ do not lie on this path, an appropriate terminal maneuver is employed. The Rutowski path is found by the following procedure.

1. Compute the initial point specific energy

$$E_1 = V_1^2/2g + h_1 \tag{170}$$

and find specific energy

$$E_2 = V_2^2/2g + h_2 \tag{171}$$

and divide the energy change $(E_2 - E_1)$ into N equal increments

2. Search at each incremental energy level

$$E_i = E_1 + i \cdot \Delta E \qquad i = 1, 2, \ldots, N \tag{172}$$

to find the point of maximum specific energy derivative, $(M_i, h_i)$ where

$$\dot{E}_i = (T_i - D_i)V_i/W_i \tag{173}$$

The $\dot{E}$ calculation is carried out for specified weight and load factor.

3. Fly a sequence of linear Mach-altitude flight increments joining the point $(M_i\ h_i)$ and $(M_{i+1}\ h_{i+1})$

A typical Rutowski path obtained from the program is illustrated in Figure 16. The initial acquisition of the Rutowski path at

$$h = h_1 + \Delta h \tag{174}$$

takes a vehicle from its initial condition to the Rutowski path with a velocity loss if this is required. The final maneuver may be either a transfer along a constant energy line from the Rutowski point at the final energy to the point $M_2h_2$. Alternatively, an altitude limit may be placed on the path such that when a Rutowski point lies above the final point, a transfer to the final point $M_2h_2$ occurs. These terminal maneuvers are sketched below.

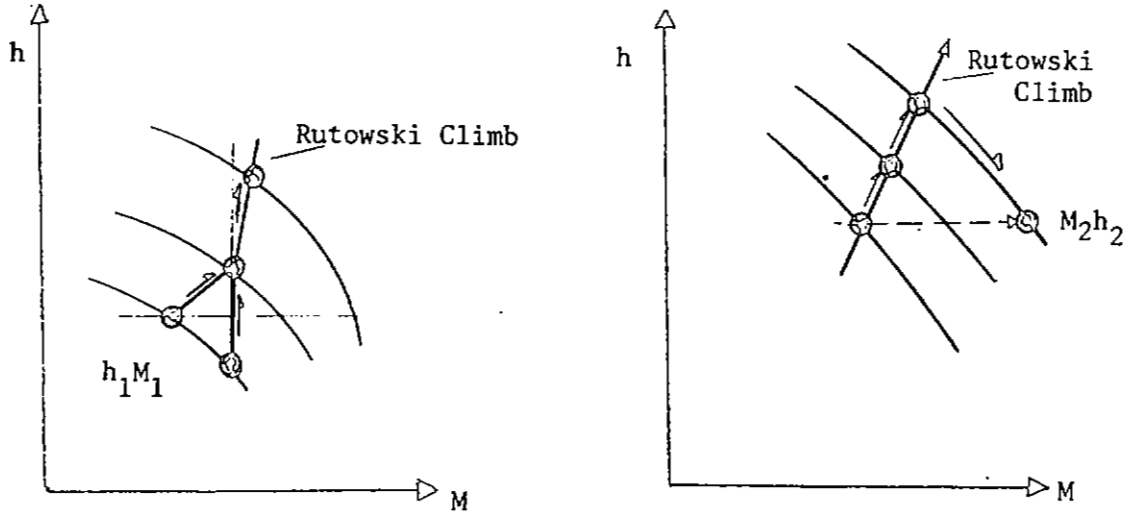


(a) Initial Maneuvers

(b) Final Maneuvers

The Rutowski path will observe both $C_{L_{max}}$ and maximum dynamic pressure constraints at the user's option. The thrust levels, vehicle weight, and load factors employed in the $\dot{E}$ calculation are specified by the user. Further details of this mission segment option may be found in Reference 2.

### 7.1.4 Maximum Rate of Climb

A maximum rate of climb path between $M_1$ $h_1$ and $M_2$ $h_2$ is generated in a similar manner to the Rutowski path of Section 7.1.3. However, in the maximum rate of climb path the search for maximum $\dot{E}$ is carried out at the constant altitudes

$$h = h_1 + i \cdot \Delta h \qquad i = 1, 2, \ldots, N \tag{175}$$

where the altitude differential $(h_2-h_1)$ has been divided into N equal increments. A typical maximum rate of climb path is shown in Figure 16.

### 7.1.5 Maximum Acceleration

A maximum acceleration path between $M_1$ $h_1$ and $M_2$ $h_2$ is generated in a similar manner to the Rutowski path of Section 7.1.3. However, in the maximum acceleration path the search for maximum $\dot{E}$ is carried out at the constant altitudes

$$M = M_1 + i \cdot \Delta M \qquad i = 1, 2, \ldots, N \tag{176}$$

where the Mach number differential $(M_2 - M_1)$ has been divided into N equal increments. A typical maximum acceleration path is shown in Figure 16. The maximum acceleration path satisfies the $C_{L_{max}}$ and maximum dynamic pressure constraints of the Rutowski path. In addition, the condition

$$\Delta E_{i+1} \geq \Delta E_i \tag{177}$$

is imposed. That is, the sequence of points, $M_i$ $h_i$ used in the acceleration will never produce a loss of specific energy. This is illustrated in Figure 17.

### 7.1.6 Minimum Fuel Paths

Minimum fuel path for given energy, altitude, and Mach number are obtained in a manner similar to Sections 7.1.3 through 7.1.5, respectively. However, the search optimization criteria on $\dot{E}$ is replaced by the criteria

$$\phi = \text{Maximum } [E/M] = \text{Max}\left[\frac{dE/dt}{dM/dt}\right] = \text{Max}\left[\frac{dE}{dM}\right] \tag{178}$$

When the search is carried out along lines of constant energy, the minimum fuel energy build up is found. When the search occurs at constant altitude, the minimum fuel climb is found. When the search occurs at constant Mach number the minimum fuel acceleration is found. All appropriate terminal maneuvers and constraints described in Sections 7.1.3 to 7.1.5 are included in the minimum fuel paths.

### 7.1.7 Maximum Range Glide

The maximum range glide path is obtained when the vehicle flies along the laws of the L/D contours tangency points to an appropriate path generating surface such as constant energy, constant altitude, or constant Mach number. The maneuvers are thus similar to those of Sections 7.1.3 to 7.1.5 using the optimization criteria

$$\phi = \text{Maximum } [L/D] \tag{179}$$

When the search is carried out along lines of constant energy, the maximum range glide for a given energy loss is found, Reference 1. When the search occurs at constant altitude, the maximum range glide for a given altitude loss is found. When the search occurs at constant Mach number, the maximum range glide for a given velocity loss is found. Some typical paths obtained from the NSEG program are illustrated in Figure 18.

### 7.1.8 Range Biased Ascents

Range biased ascents can be obtained when the vehicle flies along the locus of the T/(L-D) contours tangency points to an appropriate path generating surface. This can be seen as follows:

$$E = h + V^2/2g \tag{180}$$

and

$$m\left(\frac{dv}{dt}\right) = T - D - W \sin\gamma \tag{181}$$

Now

$$R = \int dR = \int \frac{dR}{dE}\, dE = \int \frac{dR}{dt} \cdot \frac{dt}{dE} \cdot dE \tag{182}$$

There from Equation (180)

$$R = \int \frac{V \cos\gamma \cdot dE}{\frac{dh}{dt} + \frac{V}{g} \cdot \frac{dV}{dt}}$$

$$= \frac{\cos\gamma \cdot dE}{\sin\gamma + \frac{1}{g}\frac{dV}{dt}} \tag{183}$$

But from Equation (181)

$$\frac{1}{g} \cdot \left(\frac{dV}{dt}\right) = \frac{T-D}{W} - \sin\gamma \tag{184}$$

So that

$$R = \int \frac{W \cos\gamma \cdot dE}{T-D} \tag{185}$$

Assuming that range biased ascents occur at small flight path angles with $L \simeq W$, Equation (188) becomes

$$R \simeq \int \frac{L}{T-D} \, dE \tag{186}$$

Therefore, an energy-like approximation for a range biased ascent when (L/(T-D) is a maximum at each energy level. It should be noted that when T - D = 0, no energy gain is possible; therefore, this singular condition must be avoided. In NSEG the per cent excess of thrust over drag which is acceptable is a program input.

In a manner similar to Sections 7.1.3 to 7.1.5 a range biased ascent between two energy levels occurs when the points of tangency between constant energy and T/(L-D) contours is flown. A range biased climb between two altitudes will fly the points of tangency between constant altitude and constant T/(L-D) contours. A range biased acceleration will fly the points of tangency between constant Mach number and constant T/(L-D) contours.

### 7.1.9 Range Biased Ascents Based On Range Factor

A second series of range biased ascents can be found on the basis of the range factor contours. These ascents are similar to those of Section 7.1.8 with range factor replacing T/(L-D).

## 7.2 Maximum Lift Coefficient Climb or Descent (Mission Option 2)

The maximum lift coefficient path climbs from $M_1$ $h_1$ to $M_2$ $h_2$ in N increments of altitude

$$h_i = h_1 + i \cdot \Delta h \qquad i = 1, 2, \ldots, N \tag{187}$$

At each altitude the Mach number for maximum rate of climb using the angle of attack for $C_{L_{MAX}}$ is found

$$M_i = M_{i_{MAX\ RC}} \tag{188}$$

The vehicle uses the linear Mach-altitude path path follower to climb between $M_i h_i$ and $M_{i+1}$ $h_{i+1}$.

Descents follow the same procedure as climbs, but in reverse order.

## 7.3 Radius Adjustment (Mission Option 3)

This mission segment option performs an iteration on the range of one cruise segment to make the total range over the combined mission segments $S_j$; $j = J_1, J_2 \ldots, J_N$ equal to the total range over the combined mission segments $S_k$; $k = K_1, K_2, \ldots, K_N$. That is

$$R = \sum_j R_j = \sum_k R_k \tag{189}$$

where one of the $\Delta R_j$, and only one, is being adjusted to satisfy the range equality.

## 7.4 Cruise Climb to Specified Weight (Mission Option 4)

As an aircraft cruises at the Mach number and altitude for maximum range factor, Equation (151), the weight reduces. As the weight changes, the altitude for best range factor changes while the Mach number remains approximately constant. The altitude change results from the requirement to maintain the angle of attack for maximum lift/drag ratio. Thus, as the cruise progresses the altitude increases.

The cruise may be performed in one step or it may be reduced to a sequence of five steps between latter case $W = W_1$ and $W = W_2$, Section 6.4.1. At the start of the $i^{th}$ segment in this

$$W_i = W_1 + i \cdot \Delta W \qquad i = 1, 2, \ldots, 5 \tag{190}$$

Each segment is flown at constant Mach number and lift coefficient and, hence, involves a climbing cruise. At the beginning of each cruise step the weight is instantaneously adjusted to the best altitude for the current weight.

## 7.5 Cruise Climb for Specified Distance or Time (Mission Option 5)

This mission segment option performs a cruise climb, Section 6.4 for specified distance or time. The cruise may be performed with or without range credit. This form of cruise flight is performed in one step.

## 7.6 Constant Altitude Cruise Between Two Weights, (Mission Option 6)

This mission segment performs either

1. Constant altitude, constant Mach number cruise
2. Constant altitude, constant lift coefficient cruise

between two weights $W_1$ and $W_2$. The cruise is performed in one step, see Section 6.4

## 7.7 Constant Altitude Cruise for Given Distance (Mission Option 7)

This mission segment performs either

1. Constant altitude, constant Mach number cruise
2. Constant altitude, constant lift coefficient cruise

between two distances $R_1$ and $R_2$. The cruise is performed in one step, see Section 6.4

## 7.8 Constant Altitude Cruise for Given Time (Mission Option 8)

This mission segment performs either

1. Constant altitude, constant Mach number cruise
2. Constant altitude, constant lift coefficient cruise

between two times $T_1$ and $T_2$. The cruise is performed in one step, see Section 6.4. This segment may be performed with or without range credit.

## 7.9 Buddy Refuel Cruise (Mission Option 9)

This mission segment determines the optimum in-flight refuelling point and how much fuel will be transferred. The tanker fuel off load capability is specified at three range/fuel combinations and a parabolic variation in available fuel as a function of range is assumed. That is,

$$W_f = a + bR + cR^2 \tag{191}$$

Cruise flight is assumed in any one of the three forms

1. Constant Mach number, constant lift coefficient
2. Constant Mach number, constant altitude cruise
3. Constant lift coefficient, constant altitude cruise

A maximum range for refuelling may be specified. Refuelling will occur at any point on the segment where

1. Fuel receivable is greater than or equal to fuel available

$$W_{F_R} \geq W_{F_A} \tag{192}$$

2. Distance flown is equal to maximum refuelling range

3. Minimum in-flight weight of the vehicle receiving fuel is reached where

$$W_{MIN} = W_{OWE} + W_{PL} + W_F \cdot k_F \tag{193}$$

where $k_F$ is the unusable residual fuel in the non-payload fuel. For refuelling purposes the maximum weight is taken to be the take-off weight

$$W_{MAX} = W_{TO} \tag{194}$$

## 7.10 Mach-Altitude-Weight Transfer (Mission Option 10)

This mission segment option retrieves state components at the end of flight segment i and makes them available as the initial conditions for flight segment j. The initial conditions for segment j are thus a linear transformation of the final condition of segment i,

$$\{X\}_j = [P]_{ij} \{X\}_i \tag{195}$$

Currently, the NSEG program is limited to a simple state component transfer on any combination of the three components: Mach number, altitude, or weight.

## 7.11 Alternate Mission Selection Option (Mission Option 11)

This mission option retrieves either of two mission segments on the basis of terminal Mach number, altitude or weight. Retrieval criteria may be based on any one of six possibilities:

$$\phi = \text{Min } [M_1, M_2] \tag{196}$$

$$\phi = \text{Max } [M_1, M_2] \tag{197}$$

$$\phi = \text{Min } [h_1, h_2] \tag{198}$$

$$\phi = \text{Max } [h_1, h_2] \tag{199}$$

$$\phi = \text{Min } [W_1, W_2] \tag{200}$$

$$\phi = \text{Max } [W_1, W_2] \tag{201}$$

The segment to be retained is the one which satisfies the selected performance criteria.

## 7.12 Instantaneous Weight Change (Mission Option 12)

This mission segment option permits an instantaneous change in vehicle weight, $\Delta W$. The operation

$$W_{i+1} = W_i - \Delta W \tag{202}$$

is performed.

## 7.13 Instantaneous Mach/Altitude Change (Mission Option 13)

This mission segment option provides an instantaneous change in vehicle Mach number, $\Delta M$, and an instantaneous altitude change, $\Delta h$. The new Mach number, $M_{i+1}$, and altitude, $h_{i+1}$, are specified directly; thus

$$\Delta M = M_{i+1} - M_i \tag{203}$$

$$\Delta h = h_{i+1} - h_i \tag{204}$$

## 7.14 General Purpose and Point Condition Calculation (Mission Option 14)

This mission segment option provides any of a variety of calculations described below:

1. *Best cruise altitude for given Mach number and weight based on range factor*

$$\underset{h}{\text{Max}}[RF;\ M,\ W] \tag{205}$$

2. *Ceiling for a specified rate of climb at given Mach number and weight*

$$\underset{h}{\text{Max}}[RC;\ M,\ W] \tag{206}$$

3. *Mach number for maximum lift coefficient at given weight and altitude*

$$\underset{M}{\text{Max}}[C_L;\ W,\ h] \tag{207}$$

4. *Mach number for specified lift coefficient given weight and altitude*

$$\underset{M}{\text{Find}}[C_L;\ W,\ h] \tag{208}$$

5. *Maximum endurance Mach number given altitude, weight, and maximum lift coefficient*

$$\underset{M}{\text{Min}}[\dot{W};\ W,\ h,\ C_{L_{max}}] \tag{209}$$

6. *Maximum Mach number at given weight and altitude*

$$\underset{M}{\text{Max}}[M;\ W,\ h] \tag{210}$$

7a. *Mach number for maximum rate of climb at given weight and altitude*

$$\underset{M}{\text{Max}}[RC;\ W,\ h] \tag{211}$$

7b. *Mach number for maximum rate of climb per pound of fuel at given weight and altitude*

$$\underset{M}{\text{Max}}[dh/dW;\ W,\ h] \tag{212}$$

8. *Approximate Mach number and altitude for maximum range factor given weight*

$$\underset{(M,h)}{\text{Max}}[RF;\ W] \tag{213}$$

9. *Mach number for maximum range factor given altitude and weight*

$$\underset{M}{\text{Max}}(RF;\ h,\ W] \tag{214}$$

10. *Various energy maneuverability parameters at specified load factor given Mach, altitude, and weight*

a. The required lift coefficient

b. Specific excess power

$$P_S = \dot{E} = (T-D)V/W$$

c. Specific excess power divided by fuel flow

$$P_S/\dot{W} = \dot{E}/\dot{W} = (T-D)V/(W \cdot \dot{W}) \tag{215}$$

d. Specific excess power divided by fuel flow and multiplied by fuel remaining ($\Delta E$ capability) measure

$$P_S \frac{W_F}{\dot{W}} = \frac{\dot{E}\, W_F}{\dot{W}} = \frac{dE}{dW} \cdot W_F \simeq \Delta E \tag{216}$$

e. Specific energy

$$E_S = h + V^2/2g \tag{217}$$

f. Load factor at $P_S$=0.0

g. Steady state turn radius computed as follows:

$$C_L = C_L, \text{ for given load factor}$$

Now for given bank angle, $B_A$

$$W = qSC_L \cdot \cos(B_A) \tag{218}$$

and the centrifugal force is

$$L\sin(B_A) = \frac{WV^2}{Rg} = \frac{L\cos(B_A)V^2}{Rg} \tag{219}$$

$$\therefore\ R = \frac{V^2}{g\tan \cdot B_A} \tag{220}$$

but from Equation (7.2.149)

$$\cos B_A = \frac{W}{gSC_L} \tag{221}$$

$$\therefore\ \tan B_A = \sqrt{\left(\frac{qSC_L}{W}\right)^2 - 1.0} \tag{222}$$

Substituting Equation (7.2.153) and (7.2.151)

$$R = \frac{V^2}{g}\sqrt{\frac{1.0}{\left(\frac{qSC_L}{W}\right)^2 - 1.0}} \tag{223}$$

It should be noted that this mission segment option may employ directly specified values of Mach number, altitude, and weight or these state components may be picked up from the previous mission segment termination. The option to reset Mach number, altitude, and weight from any previous segment termination is also available within the option.

## 7.15 Iteration to Fly a Specified Distance (Mission Option 15)

This mission segment option perturbs the range increment in segment i to provide a specified total range (from mission initiation) in segment j

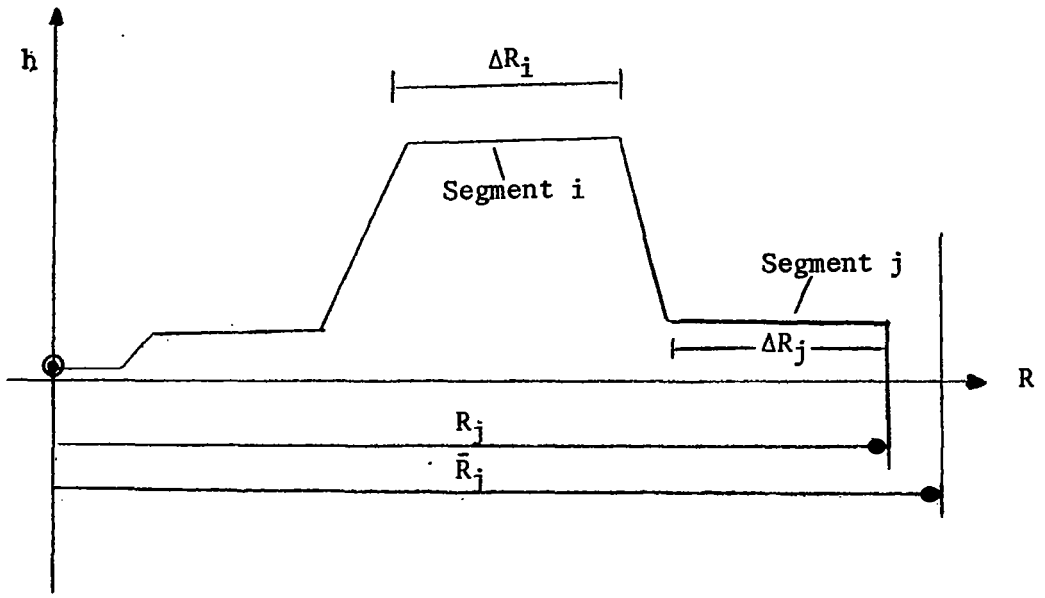


This is illustrated above where $\Delta R_i$ is perturbed to satisfy the condition

$$R_j = \bar{R}_j$$

within an error of one nautical mile.

## 7.16 Climb or Accelerate (Mission Option 16)

This mission segment option provides a climb or acceleration between two Mach number-altitude points ($M_1$ $h_1$) and ($M_2$ $h_2$). These two flight conditions must be defined in two mission segments, segment i and segment j. The climb or acceleration will then join the two points. Climb or acceleration paths may be performed in either a forward or reverse time direction. *Descents* are not permitted. The mission segment option may be performed with or without range credit.

Fuel burning decisions are made according to Mil-C rules while going from *condition 1 to 2*. Thus, fuel is burned if

$$h_2 > h_1$$

or if

$$M_2 > M_1 \quad \text{and} \quad h_2 = h_1$$

This behavior is illustrated below.

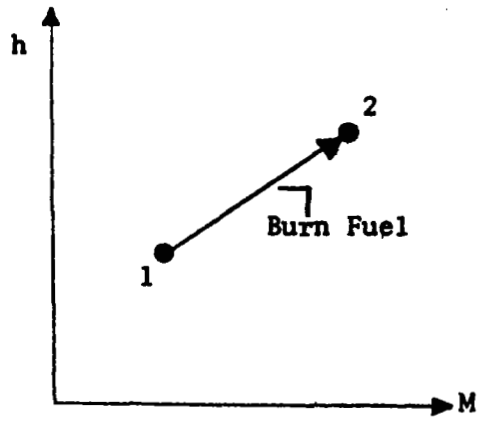


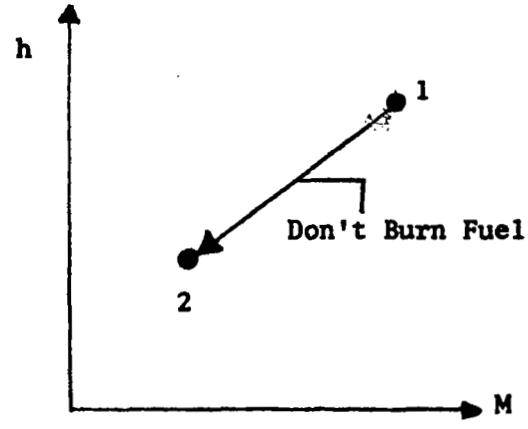


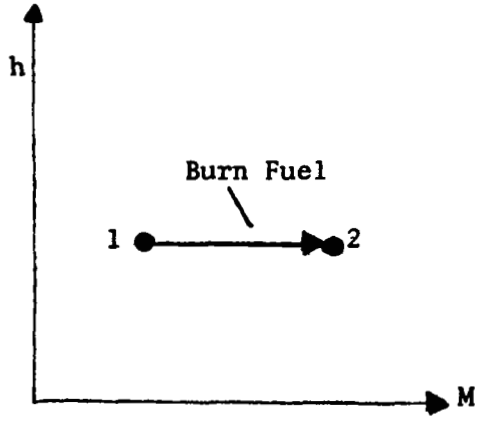


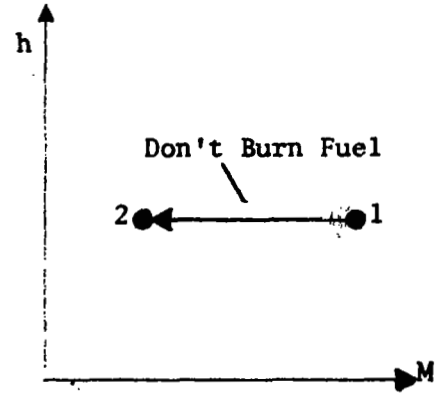

## 7.17 Fuel Weight Change (Mission Option 17)

A computed or specified fuel weight change is introduced through this mission segment option. The operation performed is

$$W_{i+1} = W_i - \Delta W \tag{224}$$

$$T_{i+1} = T_i + \Delta T \tag{225}$$

The option can be used to compute

1. Loiter fuel requirements
2. Warm up and take-off fuel
3. Combat fuel

*Take-off* fuel when computed is carried out through the take-off analysis of Section 6.1. If a detailed take-off analysis is not required the option of Section 7.18 is used. *Warm up* fuel calculation is computed for given power setting and time. *Loiter* fuel calculation is for flight at specified Mach number, altitude, weight, and a given time. *Combat* fuel calculation is for specified time or degrees of turn at a given load factor. If the degree of turn option is used, the following calculation is performed.

$$L = \bar{n} \cdot W \tag{226}$$

where $\bar{n}$ is the load factor. The centrifugal force is

$$F_R = \sqrt{L^2 - W^2} \tag{227}$$

and the turn radius is

$$R = \frac{WV^2}{g\sqrt{L^2-W^2}} \tag{228}$$

The thrust force is set to drag at the turn $C_L$

$$T = D \tag{229}$$

## 7.18 Fuel Allowance (Mission Option 20)

This mission segment option computes the fuel allowance for a specified time at

1. Given power setting
2. Given thrust/weight

## 7.19 Engine Scaling (Mission Option 21)

When using the turbojet, ramjet and/or combined engine option of Section 2.2, the engines may be resized at any point in the mission by specifying this option.

## 7.20 Generalized Iteration Control Option (Mission Option 22)

Option 22 can be used to provide an automatic iteration loop within the total mission starting and finishing with arbitrary segments input in Option 22 segment data. The purpose of the iteration is to vary a specified quantity in the starting segment until a specified quantity in the final segment specified achieves a desired value.

### 7.21 Thrust Specification in Mission Segment Options

The vehicle propulsive representations have been discussed in Section 2. In the first option of Section 2.1 there are three available maximum thrust tables, $T_{max_j}$; j = 1, 2, 3. These tables are referenced as follows:

$$\left.\begin{aligned} T_{max1} &= \text{maximum dry thrust} \\ T_{max2} &= \text{maximum wet thrust} \\ T_{max3} &= \text{maximum power} \end{aligned}\right] \qquad (230)$$

Throttling may only be used for $T_{max1}$ and $T_{max2}$. In using the various mission segment options an appropriate choice of thrust must be made. The options are

$$\left.\begin{aligned} &1.\ T = D \\ &2.\ T = \text{maximum dry} \\ &3.\ T = \text{maximum wet} \\ &4.\ T = \text{maximum power} \\ &5.\ T = \text{thrust for given power setting, dry.} \end{aligned}\right] \qquad (231)$$

In the second option of Section 2.2 either throttled or maximum power may be used.

## 8.0 FLIGHT ENVELOPE CALCULATIONS

Several gross flight envelope calculations may be performed. All flight envelope computations are subject to the conditions

$$C_L \leqslant C_{L_{lim}}\ ,\ \text{lift coefficient limit}$$

$$M \leqslant M_{lim}\ ,\ \text{Mach number limit}$$

$$q < q_{lim}\ ,\ \text{dynamic pressure limit.}$$

Propulsive and aerodynamic characteristics must be specified.

### 8.1 Climb Path History

Given an initial weight, warm up, and take-off fuel allowance, a maximum rate of climb path is performed from

$$P_1 = P_1(M_1,\ 0.0) \qquad (232)$$

to

$$P_2 = P_2(M_2, h_{MAX\ RF}) \tag{233}$$

where

$h_{MAX\ RF}$ = altitude for best range factor at $M_2$

Alternatively, $P_2$ may be selected as

$$P_2 = P_2(M_{MAX\ RF}, h_{MAX\ RF}) \tag{234}$$

The calculation is performed in ten equal altitude increments from $P_1$ to $P_2$. Climb paths are generated for N distinct weights

$$W_i = W_o + i \cdot \Delta W; \quad i = 0, 1, \ldots, N-1 \tag{235}$$

## 8.2 Endurance versus Weight at Various Altitudes

The endurance is calculated at a given altitude for the weights $W_i = W_o + i \cdot \Delta W$; $i = 1, 1, \ldots, N-1$. Mach number selected is for best endurance.

The calculation may be repeated for any number of altitudes, $h = h_o + i \cdot \Delta h$; $i = 0, 1, \ldots$.

## 8.3 Optimum Cruise Climb at Various Mach Numbers

An optimum cruise climb between $W_1$ and $W_2$ in a specified number of weight increments. The path is repeated for an array of Mach numbers and altitudes

$$M_i = M_o + i \cdot \Delta M; \quad i = 0, 1, 2, \ldots\ldots \tag{236}$$

$$h_j = h_o + j \cdot \Delta h; \quad j = 0, 1, 2, \ldots\ldots \tag{237}$$

## 8.4 Contour Presentation Capabilities

A set of point calculations (vehicle capability at given flight conditions) are carried out over a two-dimensional array of Mach-altitudes, $M_i$, $h_j$. The resulting matrix of capabilities, $F^k_{ij}$, is then supplied automatically to the NSEG contour plotting routine CONPLOT, and the contours of the function $F^k$ in the Mach-altitude plane are obtained in the form of CALCOMP, Houston plotter, or CRT display device output. At the present time twelve functions, $F^1$ to $F^{12}$, may be output in contour form. Each contour plot is described briefly below.

### 8.4.1 Specific Energy Time Derivative, $\dot{E}$, (INDMAP=1)

The specific energy time derivative is computed according to the expression

$$F^1 = \dot{E}(M, h) - (T - D)V/W \tag{238}$$

where

$\dot{E}$ = energy total time derivative

T = thrust obtained at a specified power setting or at T = D; wet, dry, or maximum power options are available

D = drag computed for a specified load factor

V = flight velocity

W = aircraft weight

Some typical energy derivative contours for a large four-engine transport are presented in Figure 19. The minimum contour shown is for the condition T - D = 0. Hence, the flight envelope is a by-product of the $\dot{E}$ map when suitable constraints such as $C_{L_{max}}$, and dynamic pressure limits are added.

### 8.4.2 Specific Energy/Fuel Flow, $\dot{E}/\dot{m}$, (INDMAP=2)

The $\dot{E}/\dot{m}$ contour presents the specific energy time derivative over the fuel flow map. Since

$$\dot{E}/\dot{m} = \frac{dE/dt}{dm/dt} = \frac{dE}{dm} \tag{239}$$

The map illustrates an aircraft's ability to convert fuel into energy at specified flight conditions.

The point calculation employed is

$$F^2 = \dot{E}/\dot{m} = (T - D)V/(W\dot{m}) \tag{240}$$

where m is the fuel flow rate. The various thrust and drag options discussed in Sections 2 and 3 may be employed to produce a family of maps. A typical example for the large subsonic transport at maximum thrust and 1g flight is shown in Figure 20.

### 8.4.3 Lift/Drag, L/D, (INDMAP=3)

Lift/drag contours present a measure of the airplane's aerodynamic efficiency. The L/D maps indicate its range capability in unpowered flight and partially reflect the cruise range capability. Mass can be produced for any specified load factor. A typical contour for the large subsonic transport in level flight is presented in Figure 21.

$$F^3 = L/D \tag{241}$$

### 8.4.4 Range Factor, $R_F$, (INDMAP=4)

Range factor contours present a measure of vehicle cruise range capability. Maps are produced for level flight with thrust equal to drag at a specified aircraft weight.

$$F^4 = R_F = \left(\frac{V}{SFC}\right)\left(\frac{L}{D}\right) \tag{242}$$

where SFC is the specific fuel consumption. The user may elect to construct maps for other than level unaccelerated flight. However, the interpretation of these charts is not clear. A typical unaccelerated flight range factor contour map for the large subsonic aircraft is presented in Figure 22.

### 8.4.5 Thrust (INDMAP=5)

The thrust map is available as a device for examining thrust input data or the thrust component of other mapped functions. The map can be obtained for wet, dry, maximum, or throttled power setting. The maximum power thrust map for the large subsonic transport is presented in Figure 23.

$$F^5 = T_{wet},\ T_{dry},\ T_{max},\ \text{or}\ T_{PS} \tag{243}$$

### 8.4.6 Drag Map (INDMAP=6)

The drag map provides a device for inspecting drag data input or the drag component of any other map. Drag maps are produced for a specified load factor. A 1g drag map for the large subsonic transport is presented in Figure 24.

$$F^6 = D_g = g^1 \tag{244}$$

### 8.4.7 Specific Fuel Consumption, SFC, (INDMAP=7)

Specific fuel consumption maps are provided as a data input inspection device or as an aid to visualizing the specific fuel consumption component of other

maps. Maps may be obtained for wet, dry, maximum, or throttled power settings. Maximum power specific fuel consumption of the large subsonic transport is presented in Figure 25.

$$F^7 = SFC_{wet},\ SFC_{dry},\ SFC_{max},\ \text{or}\ SFC_{PS} \tag{245}$$

### 8.4.8 Fuel Flow Rate, $\dot{m}$, (INDMAP=8)

The fuel flow maps are provided as a data input inspection device or as an aid to visualizing the fuel flow component of other maps. Maps may be obtained for wet, dry, maximum or throttled power settings. Maximum power fuel flow for the large subsonic transport in level unaccelerated flight is presented in Figure 26.

### 8.4.9 Specific Energy (INDMAP=9)

The specific energy map

$$F^9 = E = h + V^2/2g \tag{246}$$

is provided as a user's convenience in visualizing the trajectory points between constant energy lines and any other set of contours. An example is presented in Figure 27.

### 8.4.10 Lift/(Thrust - Drag), L/(T-D) (INDMAP=10)

The lift/(thrust - drag) contours are useful for determination of maximum range powered flight.

Assuming that maximum range flight occurs at small flight path angles

$$R \simeq \int \frac{L}{T-D}\, dE \tag{247}$$

Therefore, the energy-like approximation to maximum range flight occurs when L/(T-D) is a maximum at each energy level. It should be noted that when T - D = 0, no energy gain is possible; therefore, this singular condition must be avoided. In NSEG the per cent excess of thrust over drag which is acceptable is a program input. A typical L/(T-D) map for the large subsonic transport is presented in Figure 28.

$$F^{10} = (L/CT\text{-}D)_{\text{specified excess thrust}} \tag{248}$$

### 8.4.11 Turn Radius (INDMAP=11)

Turn radius maps give a gross indication of aircraft's combat capability. Turn radius is computed by equating the aircraft's lift capability in steady state of decelerating flight using the following expression

$$F^{11} = R = w \left(\frac{V^2}{g}\right) \left[\frac{1.0}{(qSC_L)^2 - W^2}\right]^{1/2} \quad (249)$$

where $C_L$ is determined so that (a) thrust equals drag for steady state flight and (b) $C_L$ equals $C_L$ maximum for minimum instantaneous turn radius.

Typical radius of turn map for the subsonic transport are presented in Figure 29.

### 8.4.12 Time to Turn (INDMAP=12)

Time to turn through 180 degrees is presented as a supplement to the turn radius map. When the minimum instantaneous turn radius calculation is employed, the maps do not give a true time to turn. They merely indicate how long a time the aircraft would take to turn *if it could maintain its current turn rate.* When steady state turns are considered, true time to turn is obtained *which will frequently be much longer than is required for a decelerating turn.* Typical time to turn maps for the subsonic transport are illustrated in Figure 30.

$$F^{12} = \pi R/V \quad (250)$$

*REFERENCES:*


1. Rutowski, E. R., "Energy Approach to the General Aircraft Performance Problem," Journal of the Aeronautical Sciences, March 1954.

2. Raybould, B., "Approximate Trajectories for Maximum Range," Journal of the Aeronautical Sciences, June 1963.

3. Hague, D. S. and Jones, R. T., Energy Maneuverability Options for Mission Segment Analysis Program--NSEG, TN-149, Aerophysics Research Corporation, April 1972.

Hi-Lo-Lo-Hi Radius Mission

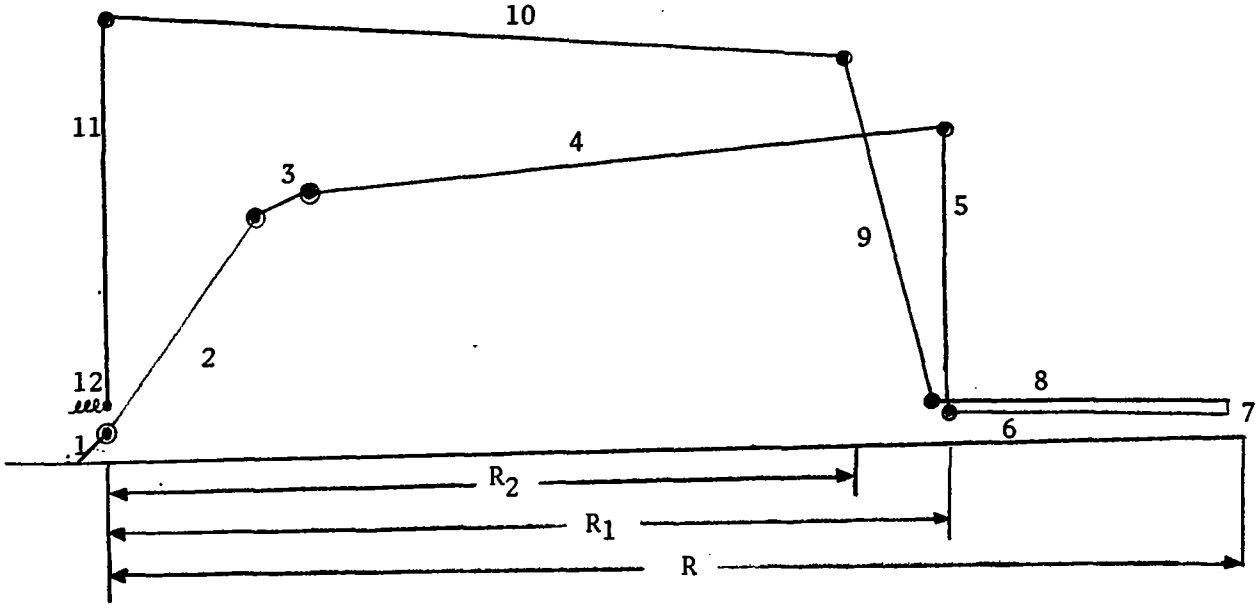


1. Take-off
2. Maximum rate of climb to best cruise altitude given weight and Mach number
3. Constant $C_L$ climb to best cruise altitude for new weight and Mach number
4. Breguet cruise to given range, R
5. Instantaneous state change to dash Mach number and altitude
6. Constant Mach number-altitude cruise to total range, R
7. Drop ordnance, instantaneous weight change
8. Constant Mach number-altitude return cruise to given weight
9. Maximum rate of climb to given Mach number-altitude
10. Breguet cruise to given weight
11. Instantaneous state change to best endurance Mach number for given altitude and weight
12. Loiter for given time

FIGURE 1. TYPICAL NSEG MISSION PROFILE

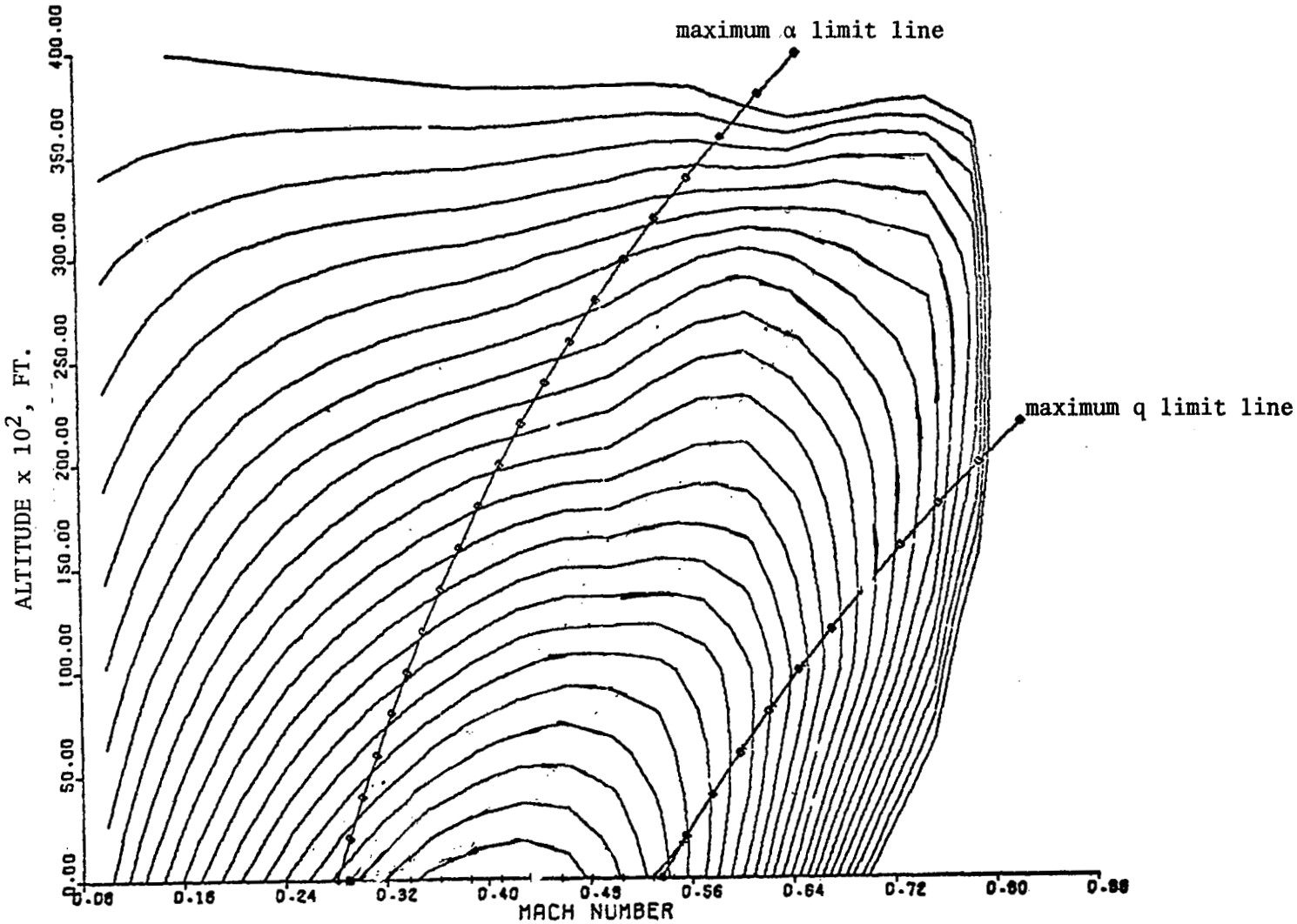


FIGURE 2. TYPICAL FLIGHT POINT PERFORMANCE MAPS
(SPECIFIC ENERGY AT VARIOUS LOAD FACTORS, WEIGHTS, AND THRUSTS)
WITH TRAJECTORY LIMITS OVERLAID

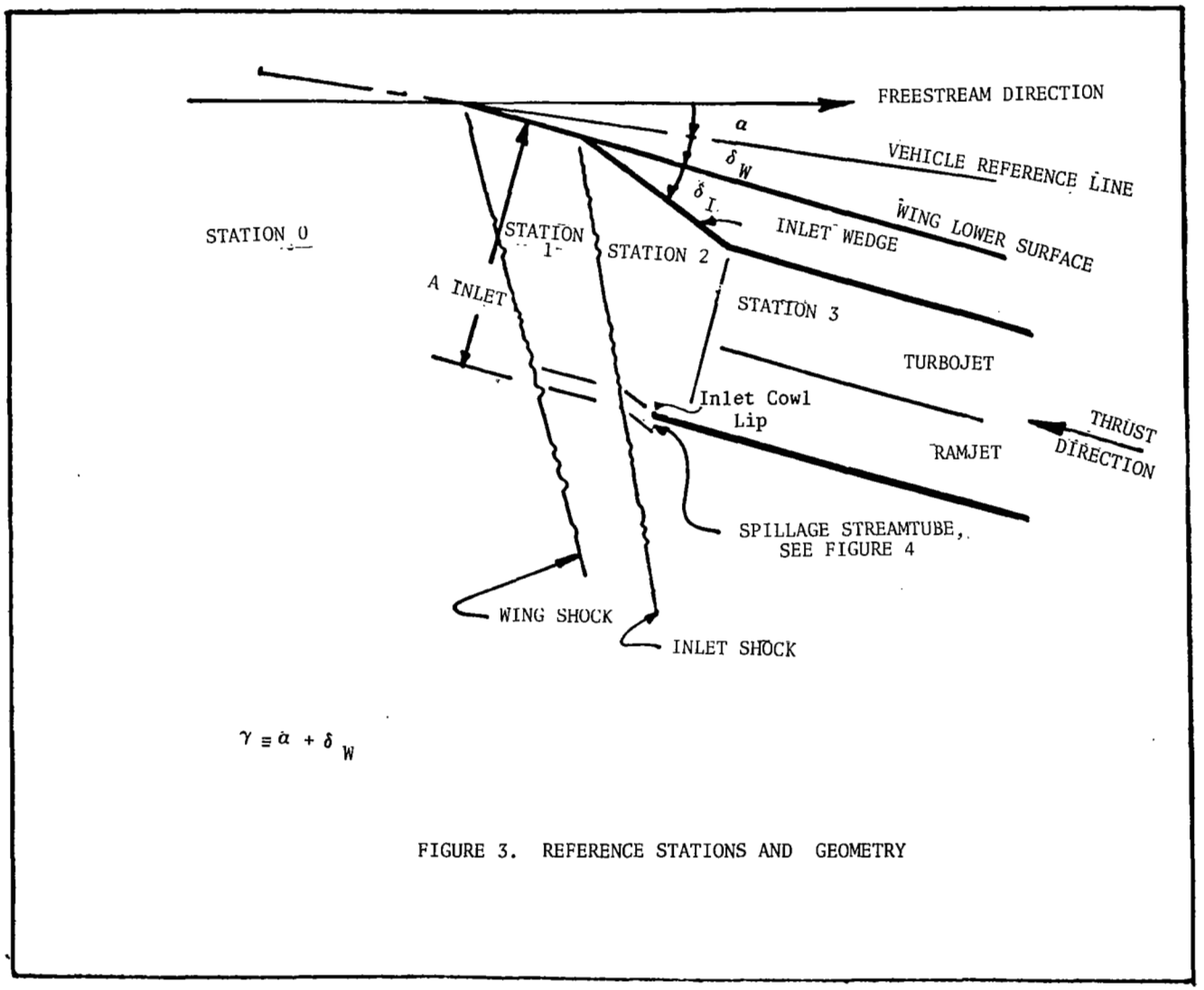


FIGURE 3. REFERENCE STATIONS AND GEOMETRY

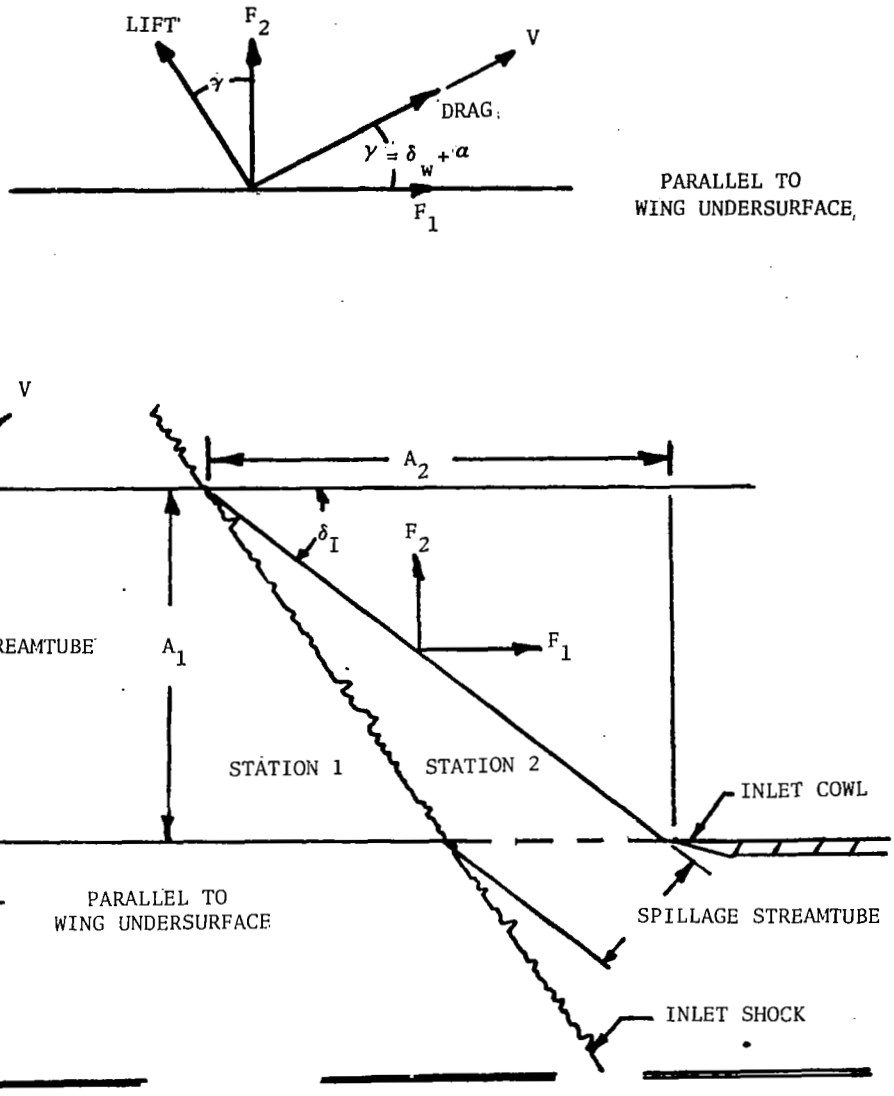


$A_1$ = SPILLED AIRFLOW/$\rho_1 V_1$

$A_2 = A_1/\text{Tan}\ \delta_I$

$F_1 = (P_2 - P_0)A_1$ $\qquad F_2 = (P_2 - P_1)A_2$

$L_{SPILL} = F_2 \cos\gamma - F_1 \sin\gamma$ $\qquad D_{SPILL} = F_1 \cos\gamma + F_2 \sin\gamma$

FIGURE 4. SPILLAGE LIFT AND DRAG COMPUTATIONS

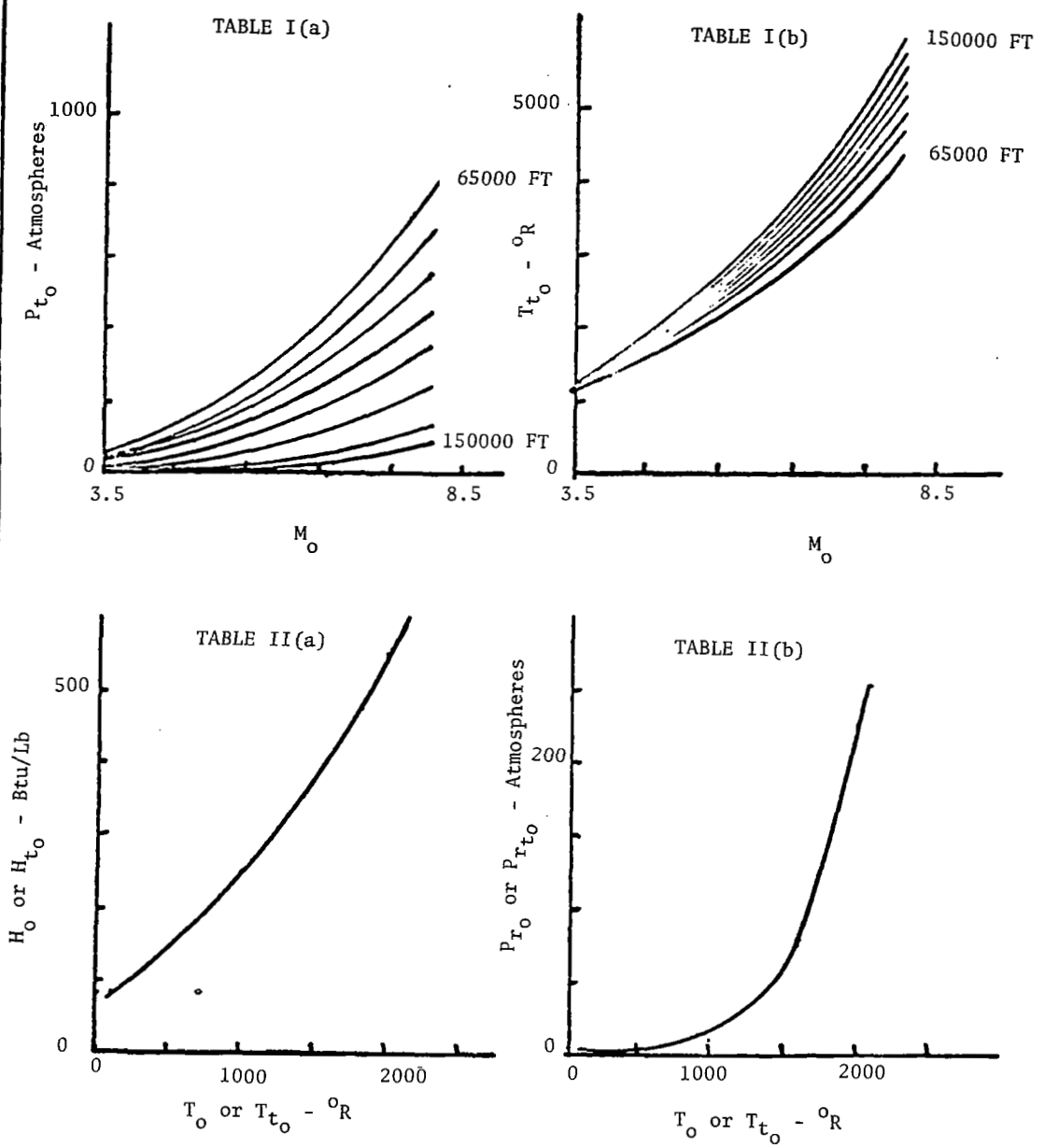


FIGURE 5. TYPICAL TABLE DATA

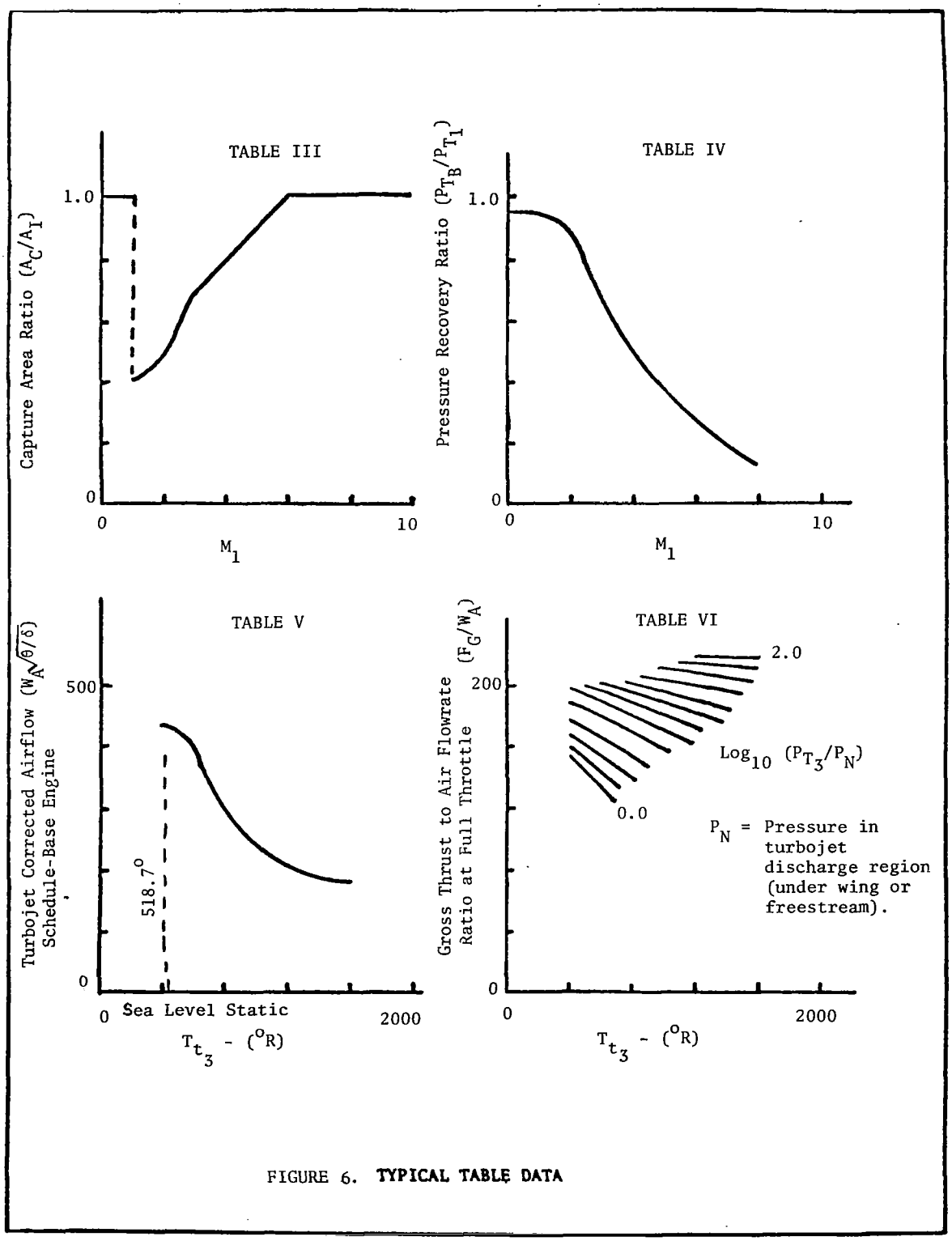


FIGURE 6. **TYPICAL TABLE DATA**

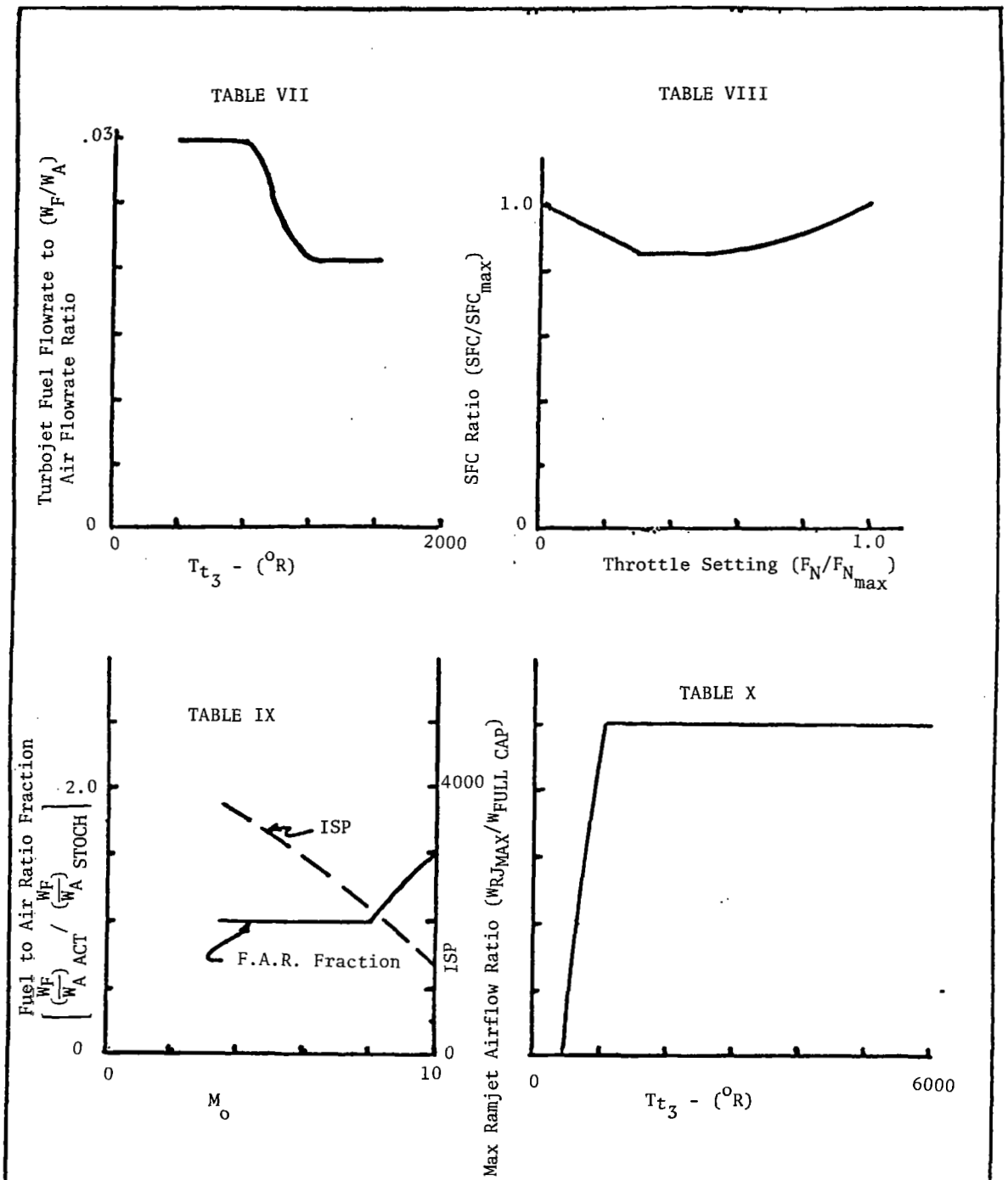


FIGURE 7. **TYPICAL TABLE DATA**

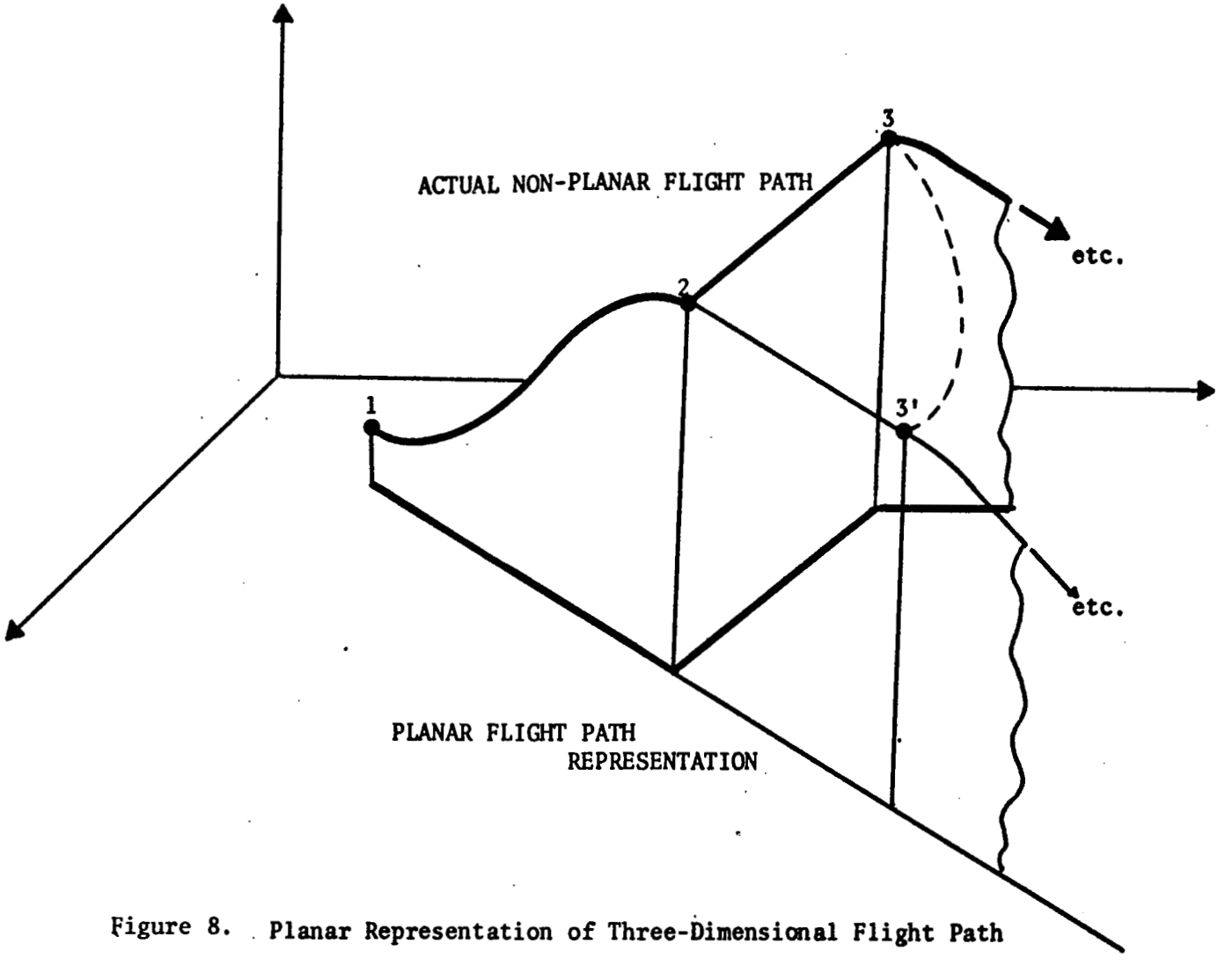


Figure 8. Planar Representation of Three-Dimensional Flight Path

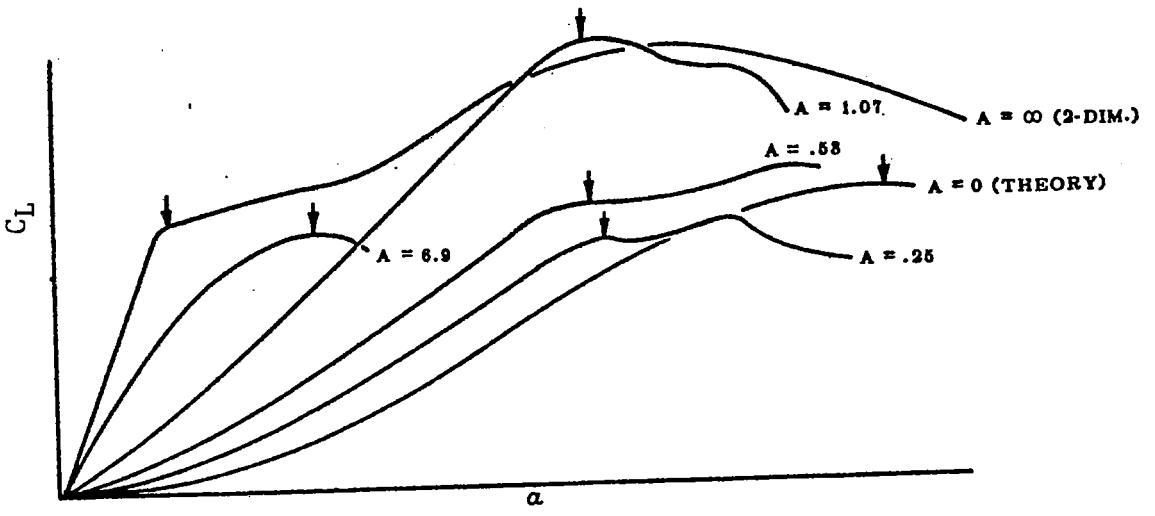


FIGURE 9. TYPICAL FIRST PEAKS IN LIFT COEFFICIENT VERSUS ANGLE OF ATTACK

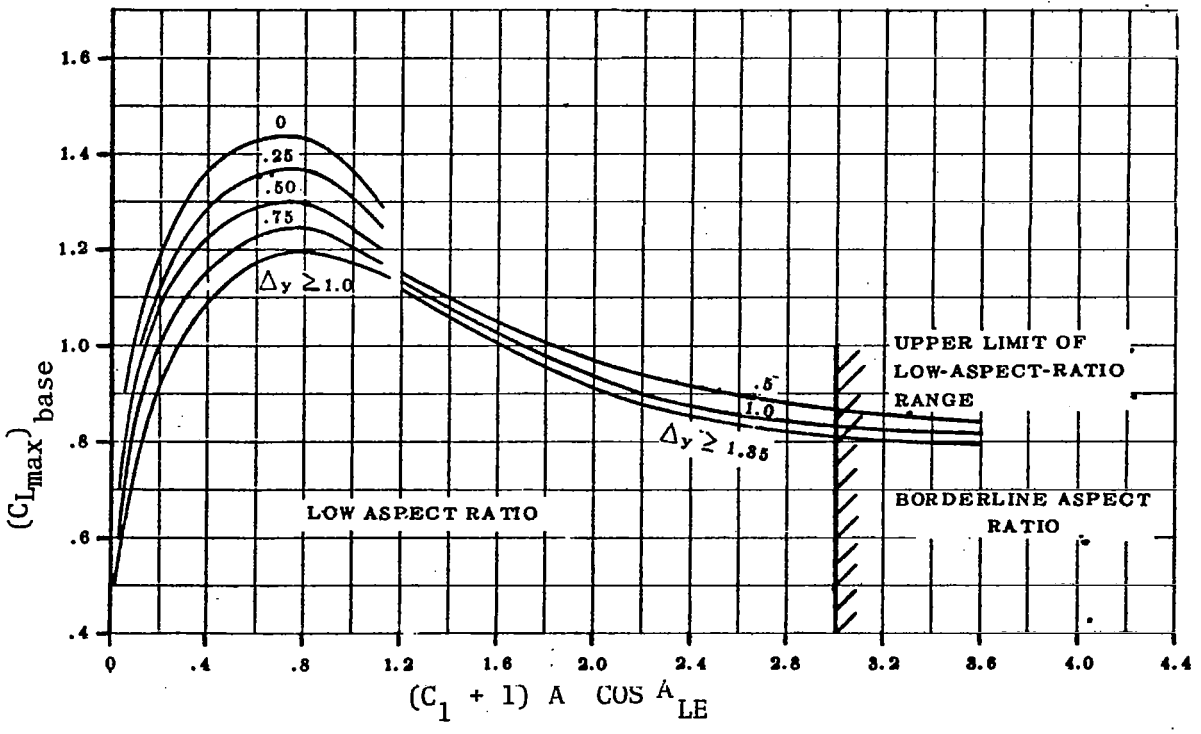


FIGURE 10. SUBSONIC MAXIMUM LIFT OF WINGS WITH POSITION OF MAXIMUM THICKNESS BETWEEN 35 AND 50 PER CENT CHORD

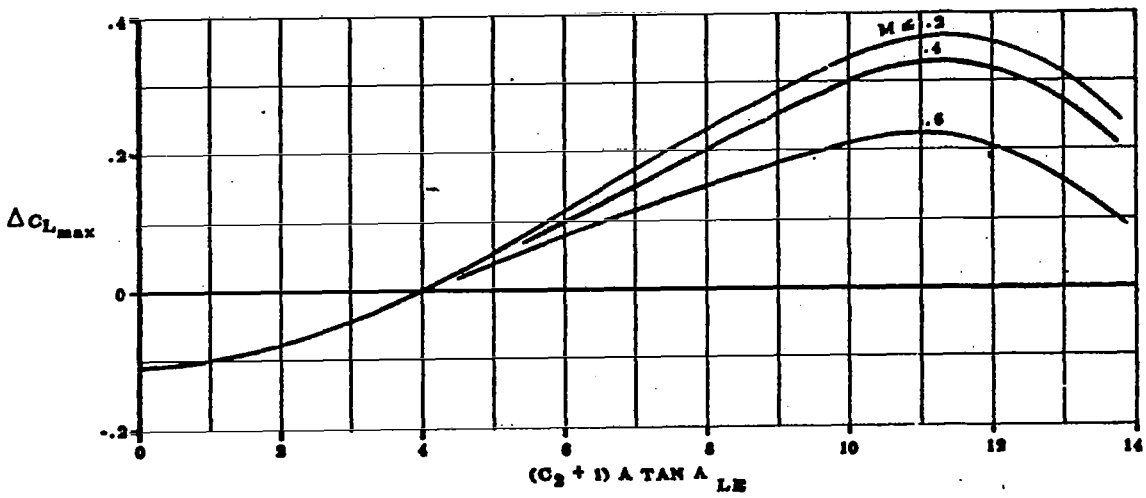


FIGURE 11. SUBSONIC MAXIMUM LIFT INCREMENT FOR LOW ASPECT RATIO WINGS

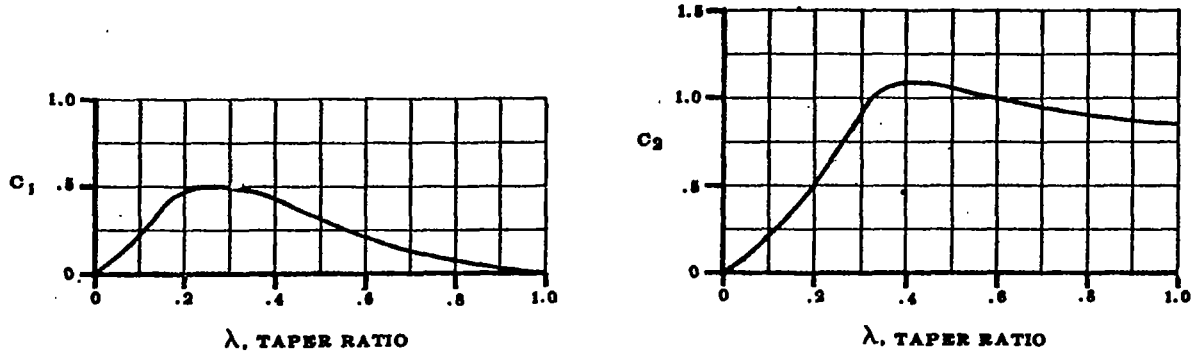


FIGURE 12. TAPER RATIO CORRECTION FACTORS

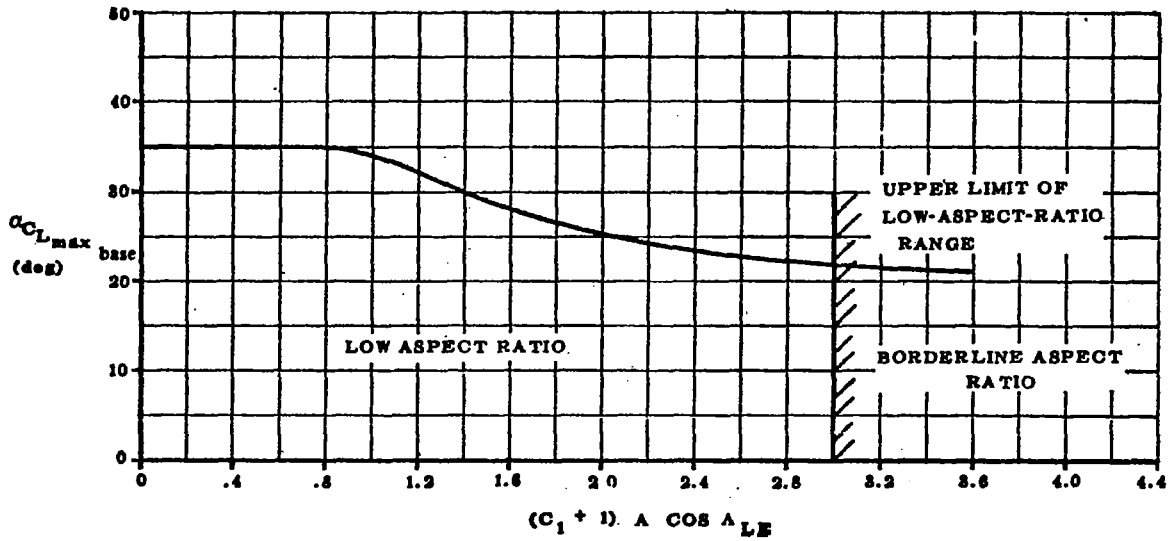


FIGURE 13. ANGLE OF ATTACK FOR SUBSONIC MAXIMUM LIFT OF LOW ASPECT RATIO WINGS

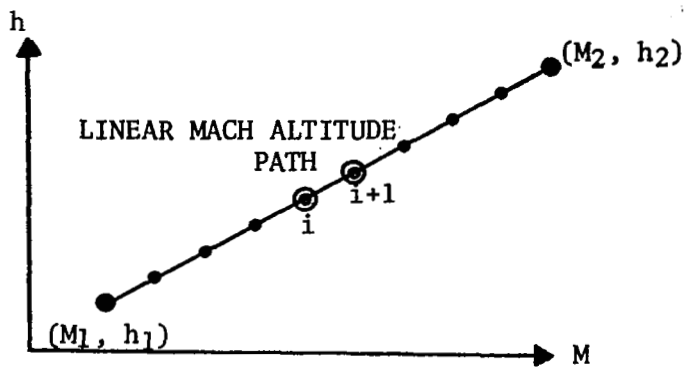


Figure 14. Linear Mach Altitude Mach Segment

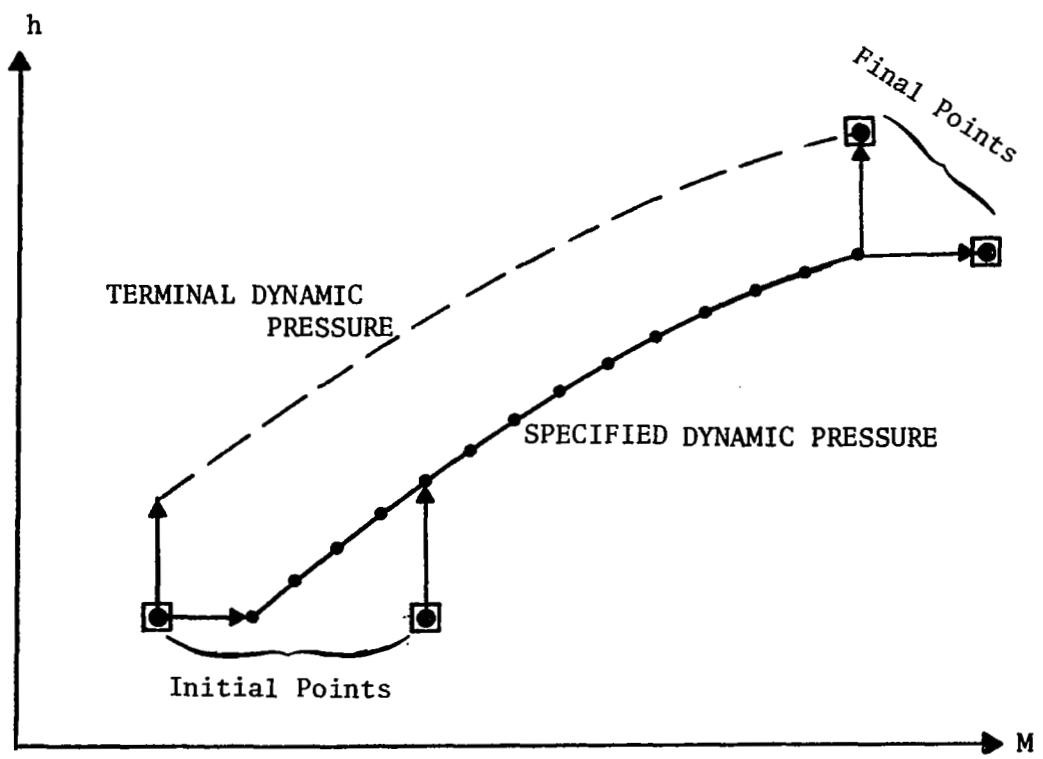


Figure 15. Constant Dynamic Pressure Segment Illustrating Treatment of End Points

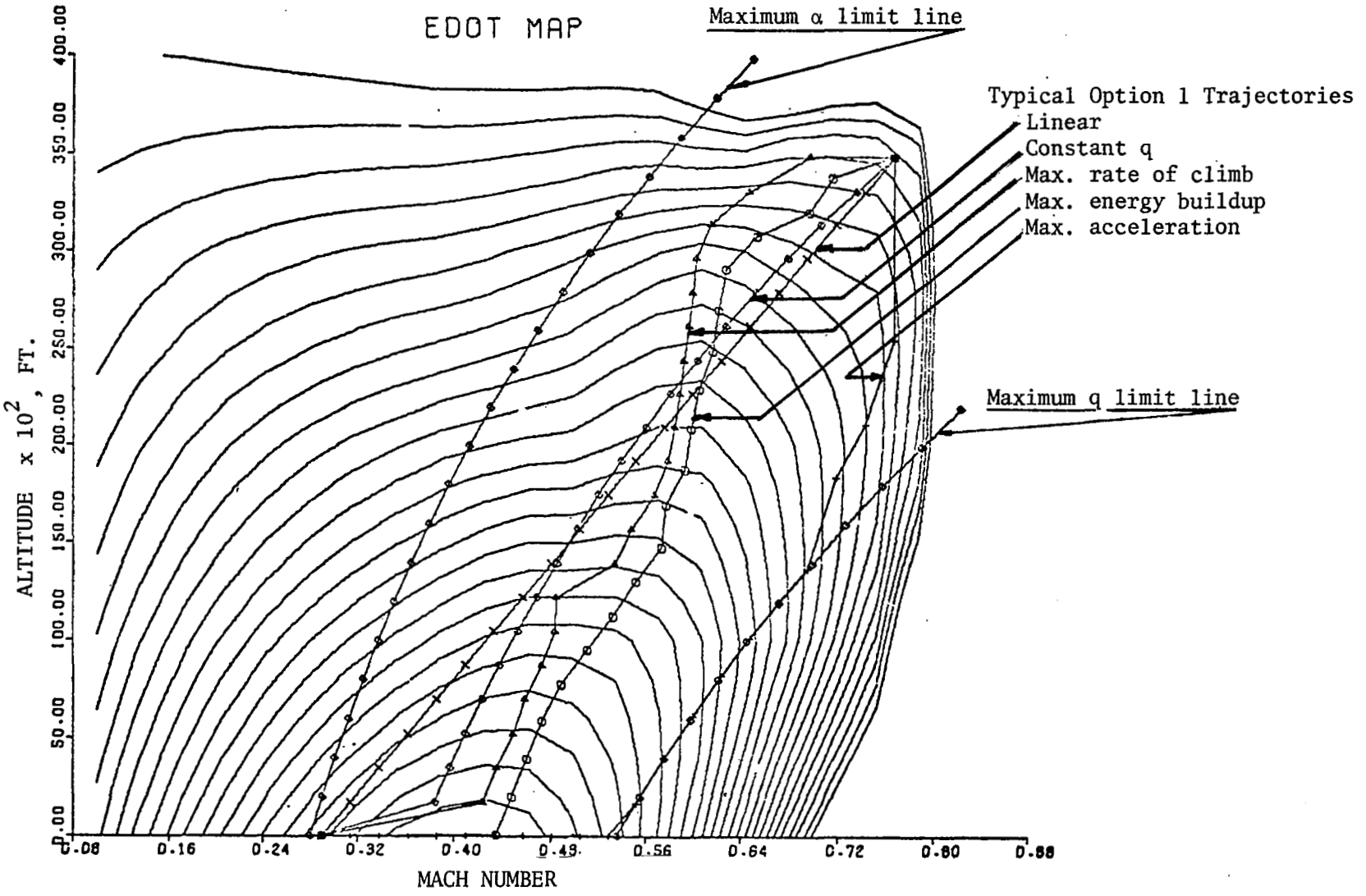


FIGURE 16. TYPICAL NSEG CLIMB PATHS DISPLAYED ON AIRCRAFT $\dot{E}$ CONTOURS

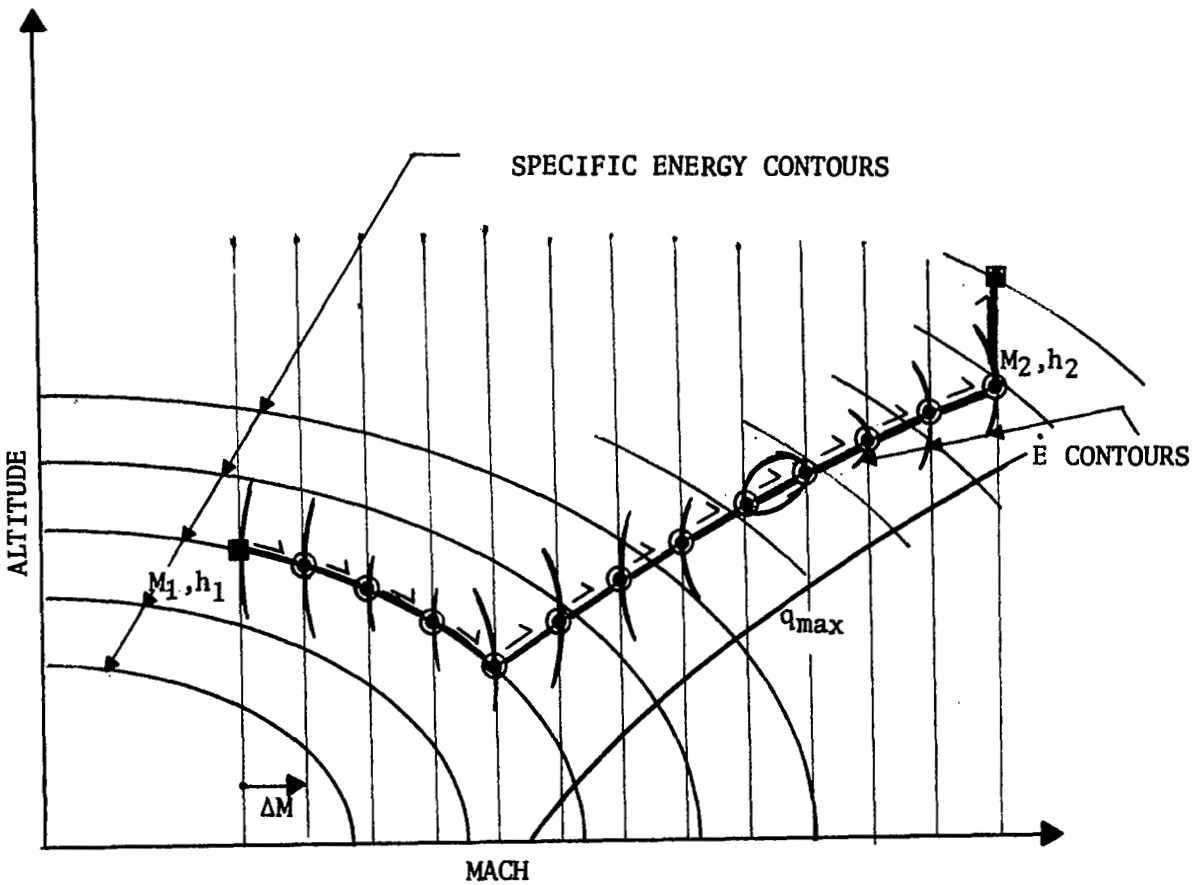


Figure 17. Energy Constraint Imposed on Maximum Acceleration Path

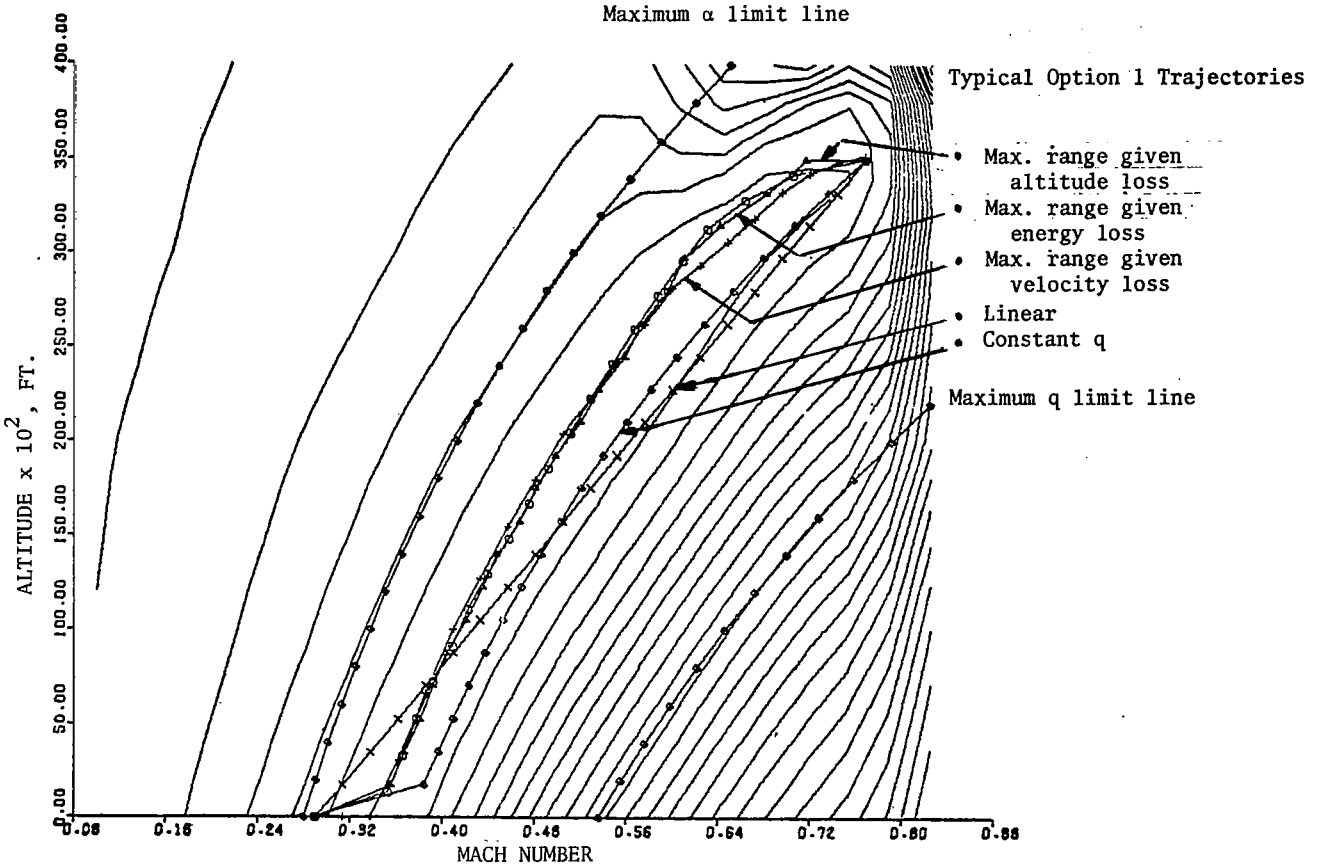


FIGURE 18. LIFT/DRAG MAP WITH DESCENT PATHS AND LIMITS SUPERIMPOSED

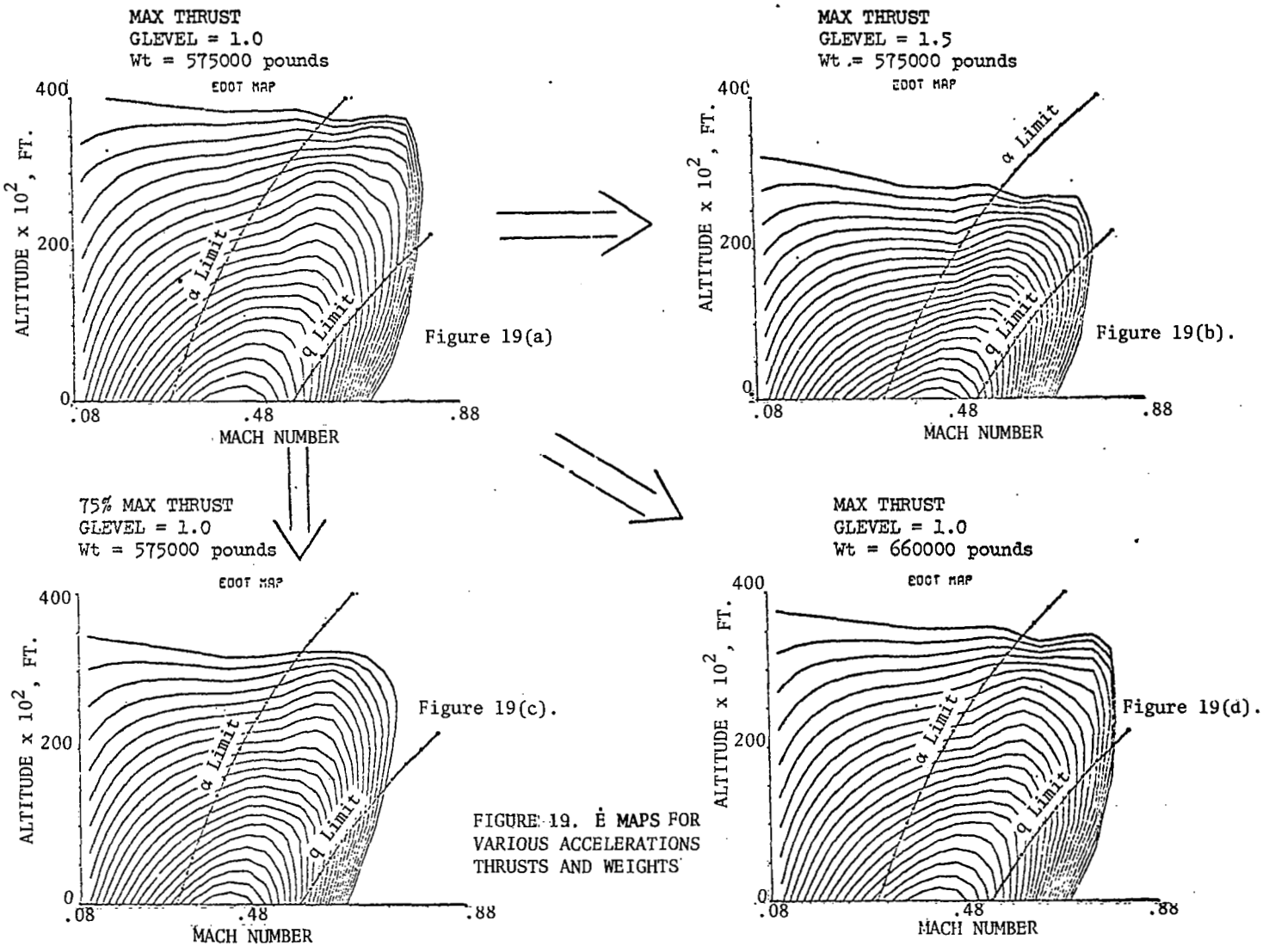


FIGURE 19. $\dot{E}$ MAPS FOR VARIOUS ACCELERATIONS THRUSTS AND WEIGHTS

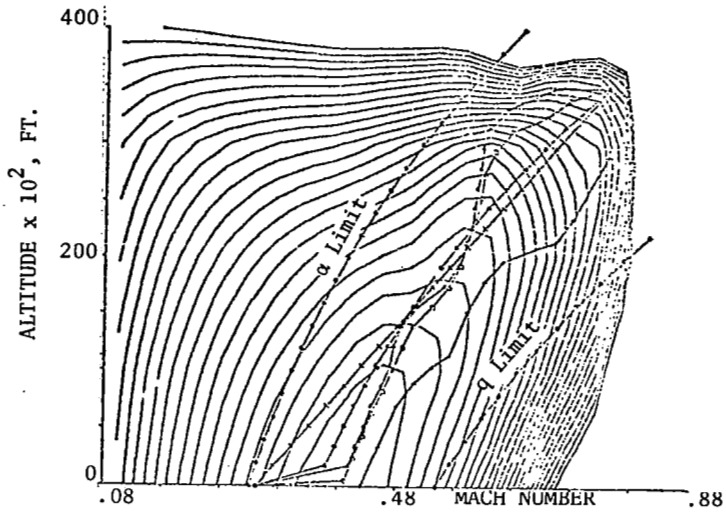


FIGURE 20. EDOT/MDOT MAP (COMPUTER DRAWN)

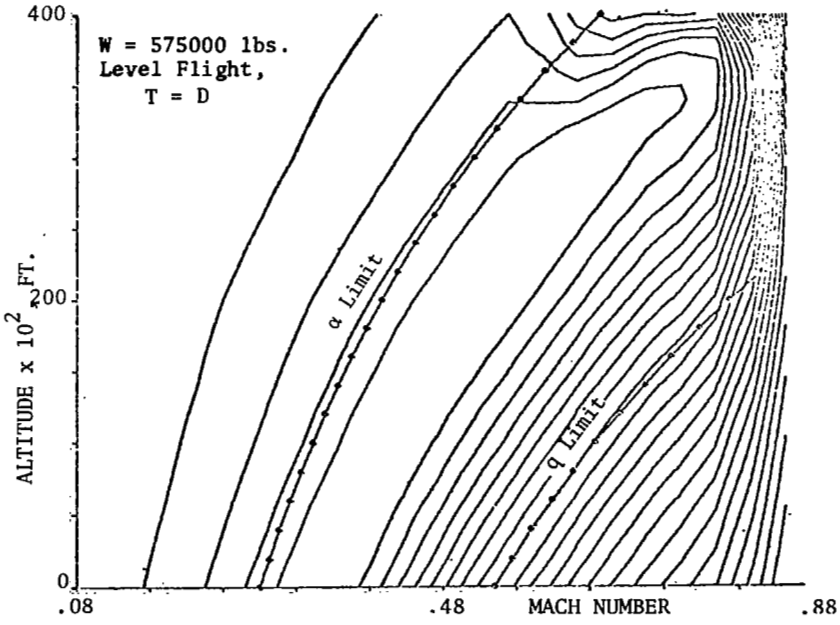


FIGURE 21. LIFT/DRAG MAP (COMPUTER DRAWN)

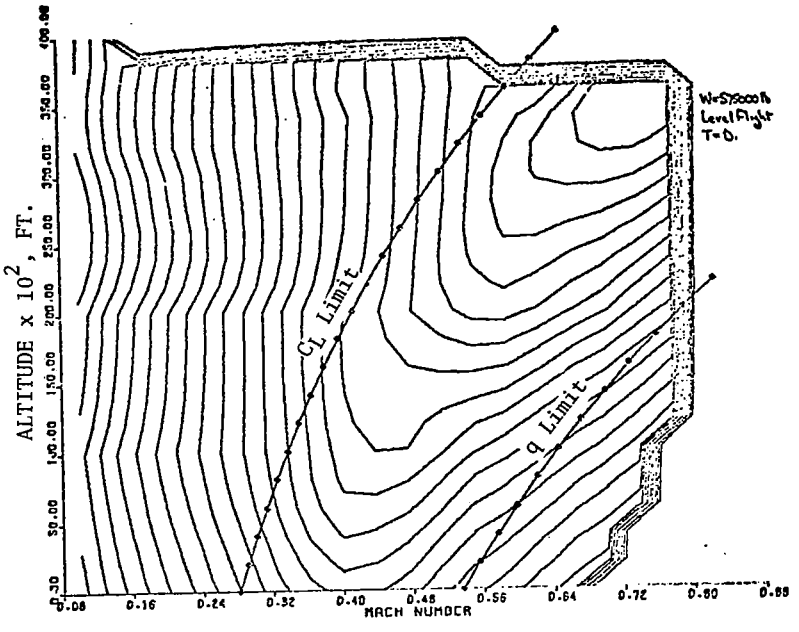


FIGURE 22. RANGE FACTOR MAP (COMPUTER DRAWN)

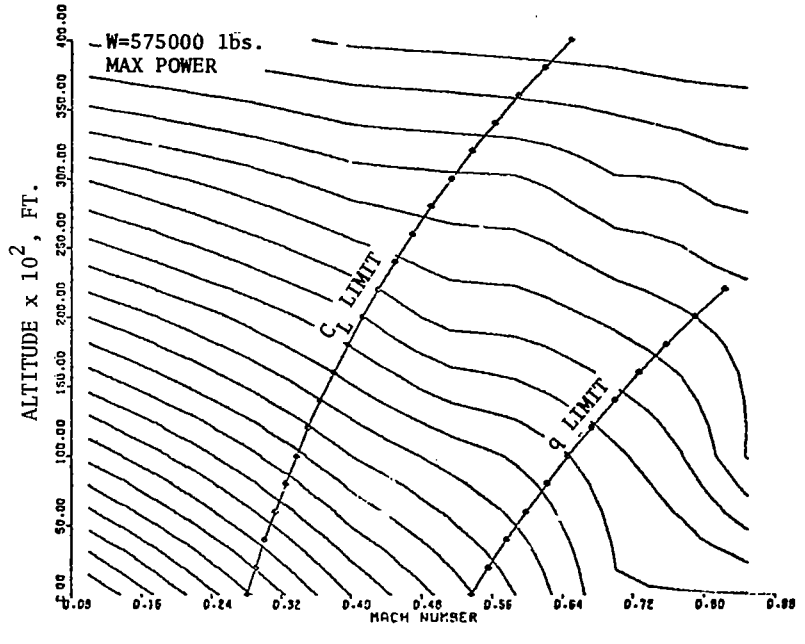


FIGURE 23. THRUST MAP (COMPUTER DRAWN)

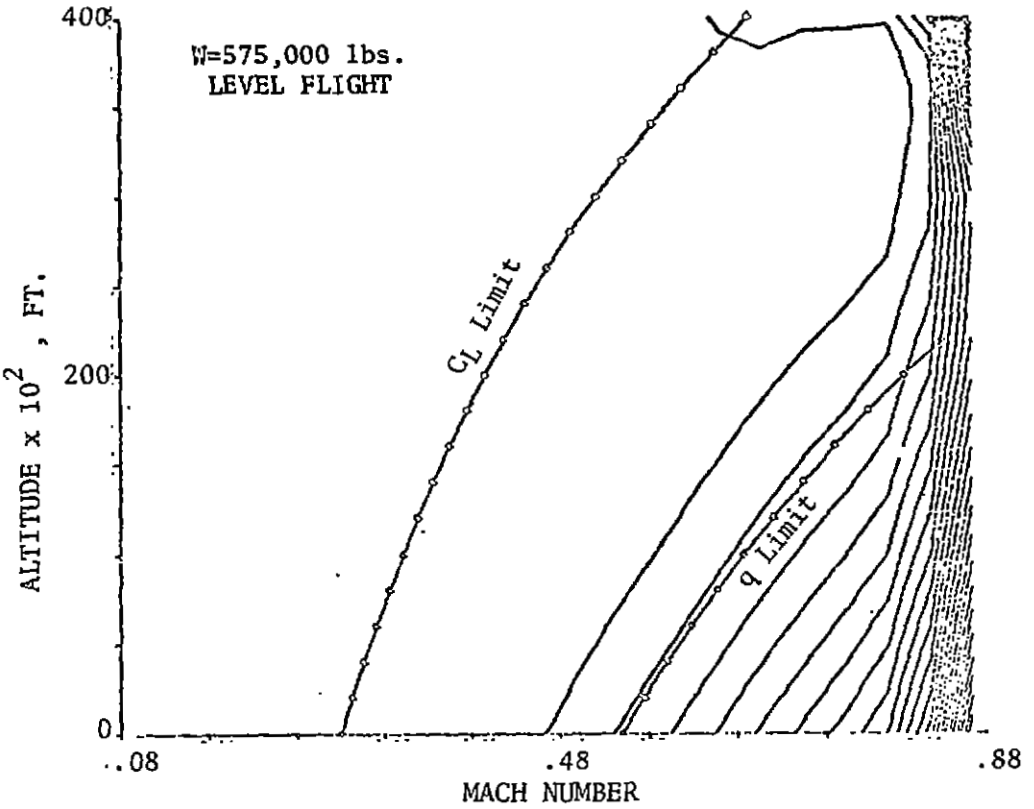


FIGURE 24. DRAG MAP (COMPUTER DRAWN)

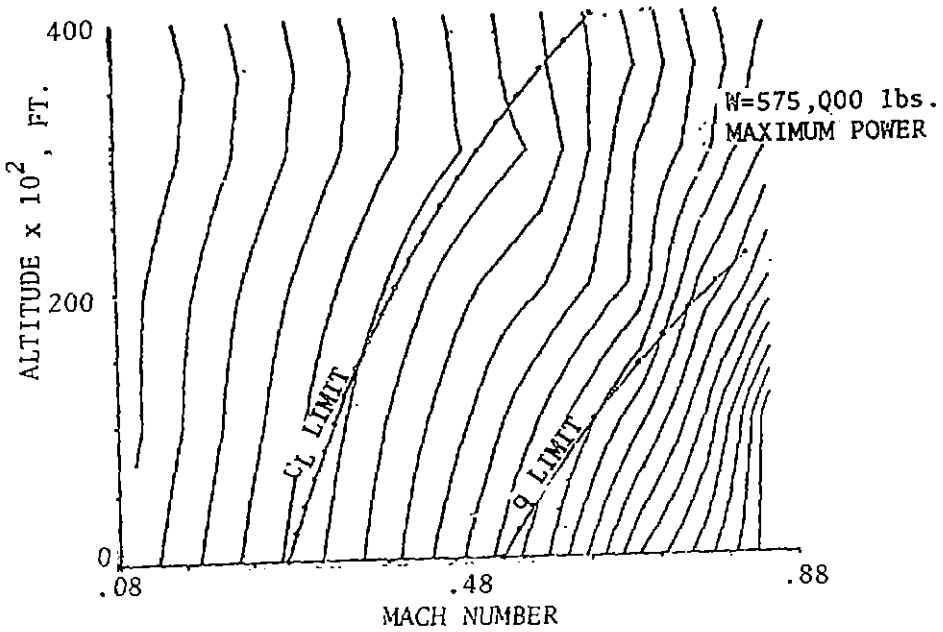


FIGURE 25. SPECIFIC FUEL CONSUMPTION MAP (COMPUTER DRAWN)

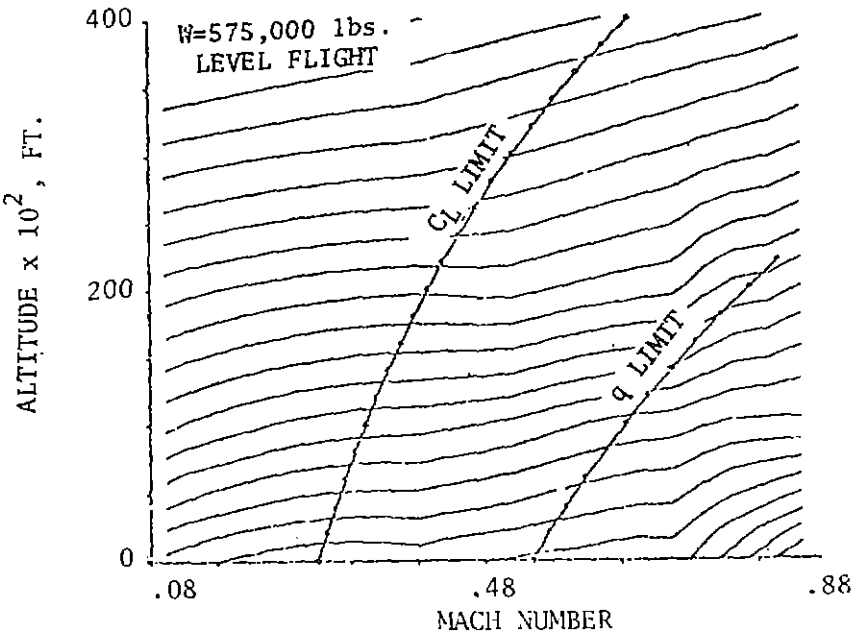


FIGURE 26. FUEL FLOW RATE MAP (COMPUTER DRAWN)

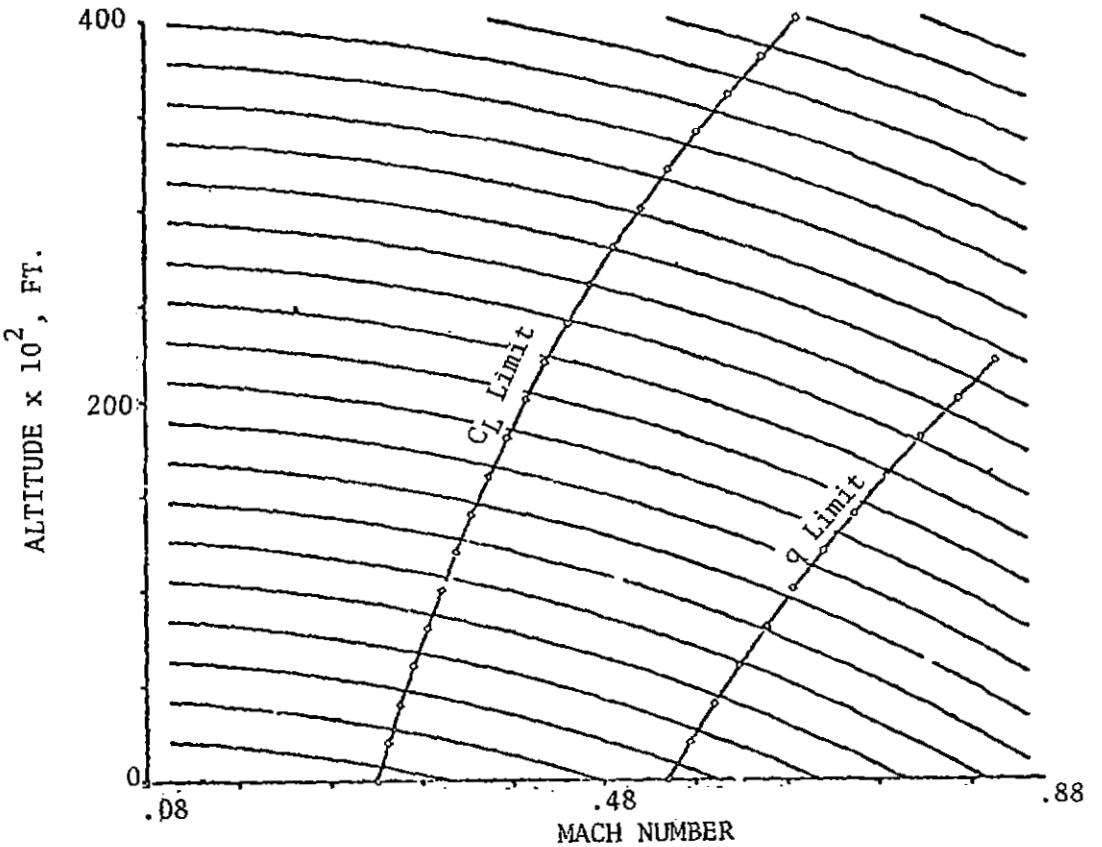


FIGURE 27. SPECIFIC ENERGY MAP (COMPUTER DRAWN)

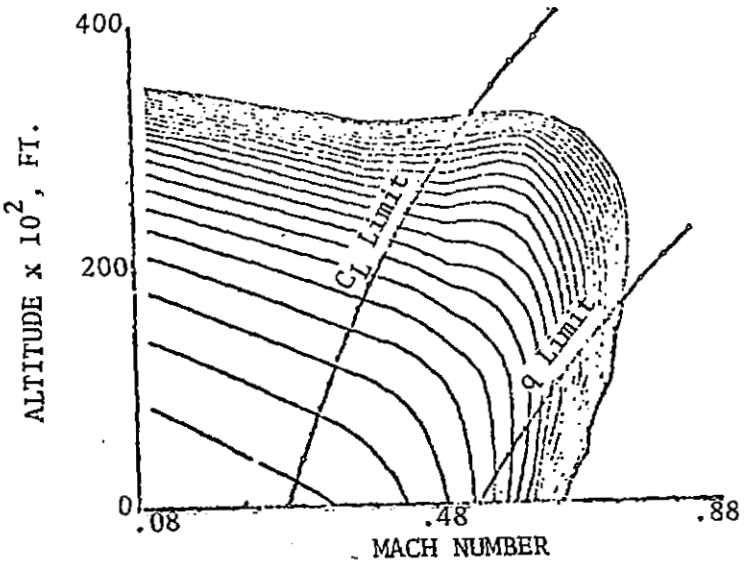


FIGURE 28. LIFT/(THRUST-DRAG) (COMPUTER DRAWN)

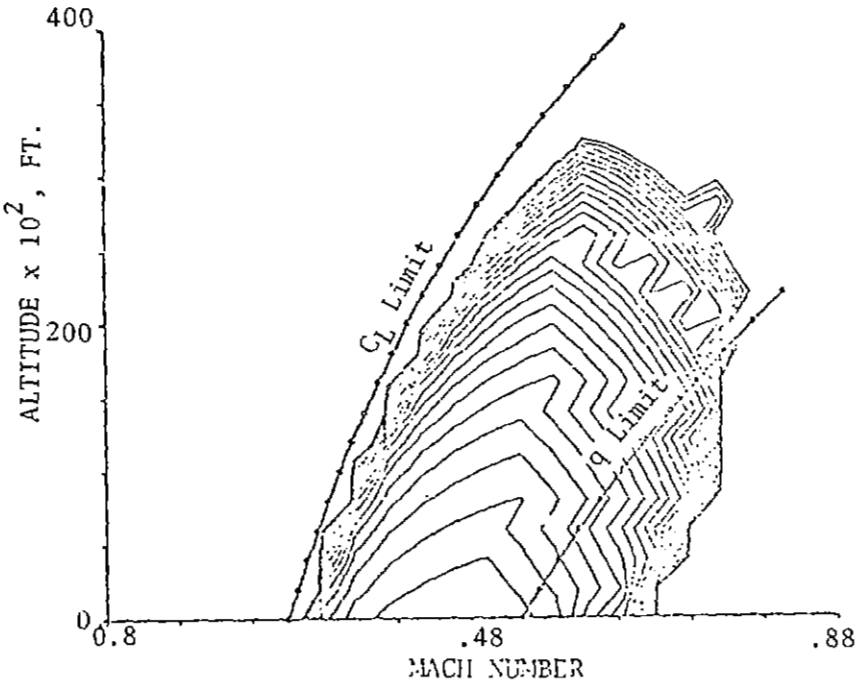


FIGURE 29. RADIUS OF TURN MAP (COMPUTER DRAWN)

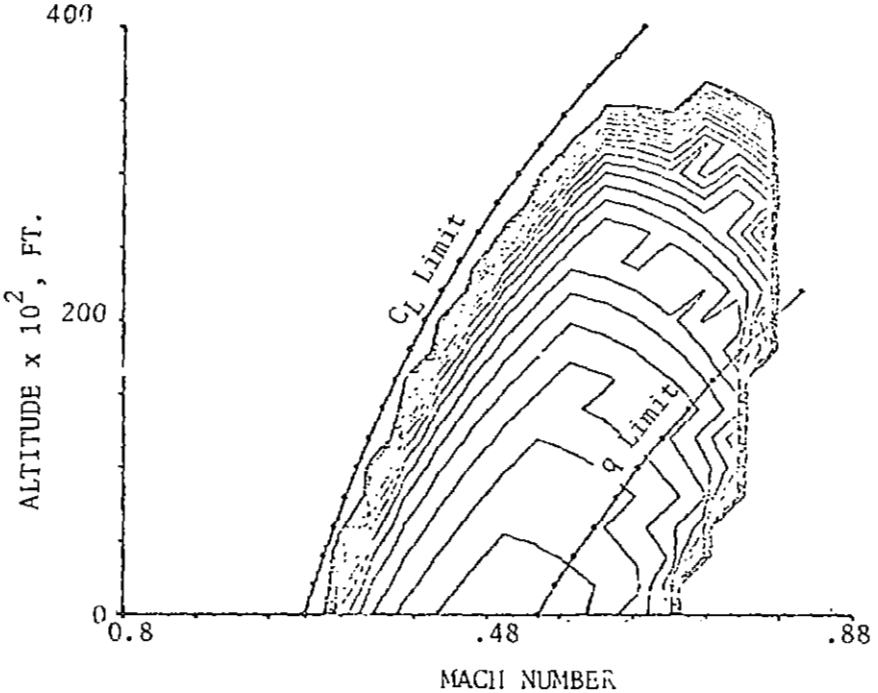


FIGURE 30. MAP OF TIME TO TURN 180 DEGREES (COMPUTER DRAWN)